

Environmental impact of tidal power in the Eastern Scheldt Storm Surge Barrier



Prepared for:

DMEC WP3.7, Kansen voor West: UP16-00127

Deltares project: 11200119

OTP PROJ-00275, Stimulus: UP-16-01097

Deltares project: 11200444

Environmental impact of tidal power in the Eastern Scheldt Storm Surge Barrier

Anton de Fockert and Arnout Bijlsma

11200119-000

Title

Environmental impact of tidal power in the Eastern Scheldt Storm Surge Barrier

Project

11200119-000

Attribute

11200119-000-HYE-0006

Pages

36

Keywords

Tidal power, tidal turbines, Eastern Scheldt Estuary

Summary

At the end of 2015, a first of its kind tidal power plant was installed in Gate 8 of the Roompot Section of the Eastern Scheldt Storm Surge barrier. This tidal power plant consists of 5 tidal turbines. To assess the environmental impact of this tidal power plant, several detailed studies have been conducted to analyse potential effects of the turbines on:

- 1 tidal ranges in the Eastern Scheldt, by analysing long-term water level data,
- 2 the discharge capacity of the barrier by means of current measurements and detailed numerical simulations,
- 3 the large-scale flow patterns in the Roompot Section,
- 4 the local flow field, especially near the bed protection,
- 5 the morphology in the Eastern Scheldt by investigating sedimentation and erosion processes of intertidal areas.

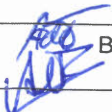

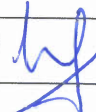
The study subjects described above were investigated within the DMEC and OTP research projects. For each study, a separate report has been written. The present report summarizes the conclusions of the different reports and combines the knowledge that has been gathered in the research programs to obtain an integral view on the environmental effects of the tidal energy extraction in the Eastern Scheldt.

The tools developed in the investigations seem to be adequate to address the impact of tidal turbines on the various aspects of flow velocities and turbulence for which RWS expressed its concern. Though the effects of the tidal power plant in Roompot 8 (operating under a limited head difference condition of -60/+80 cm) are fairly mild, the extrapolation of the results of the investigated cases of -20/+20 cm and -32/+55 cm for Gate Roompot 8 to the anticipated increase of the operational head difference of -90/+90 cm is not feasible. It is recommended to perform additional simulations for this particular case to confirm that there is not the smallest risk involved for the barrier. Furthermore, when the design of the tidal power plant in Gate Roompot 10 is changed when compared to Roompot 8, new simulations for this will be required as well.

References

DMEC WP 3.7, Kansen voor West: UP16-00127

Oosterschelde Tidal Power PROJ-00275, Stimulus ref: UP-16-01097

Version	Date	Author	Initials	Review	Initials	Approval	Initials
0 _{draft}	Aug. 2018	Anton de Fockert Arnout Bijlsma		Bas van Vossen		Wiel Tilmans	
1 _{final}	Feb. 2019	Anton de Fockert Arnout Bijlsma		Bas van Vossen		Wiel Tilmans	

Status

final

Table of contents

1	Introduction	1
1.1	Background	1
1.2	Requirements of the permits	1
1.3	Objective and study subjects	2
1.4	Research frameworks	2
1.4.1	DMEC project	2
1.4.2	OTP project	3
1.4.3	NWO The New Delta project on tidal turbines in the Eastern Scheldt Barrier	3
1.4.4	Project team	3
2	Subject 1: Effect on water levels	5
2.1	Approach	5
2.2	Regression analysis tidal range Roompot Binnen and Roompot Buiten	5
2.3	Long-term variation	5
2.4	Conclusion	7
3	Subject 2: Effect on discharge capacity of the barrier	8
3.1	Subject 2A: Analysis of current measurements	8
3.1.1	Measurement setup	8
3.1.2	Analysis	10
3.1.3	Discharge coefficient	12
3.1.4	Conclusions	12
3.2	Subject 2B: CFD simulations	13
3.2.1	Characteristics of the CFD model	13
3.2.2	Model validation	15
3.2.3	Discharge coefficient	18
3.3	Conclusions	18
4	Subject 3: Changes in large-scale flow patterns	19
4.1	Brief model description	19
4.2	Flow fields	21
4.3	Conclusion	23
5	Subject 4: Impact on bed protection	24
5.1	Changes in flow patterns due to the turbines	24
5.2	Flow fields near the bed at 100m from the barrier	26
5.3	Conclusions	28
6	Subject 5: Morphological effects in the Eastern Scheldt	29
6.1	Roll-out scenarios	29
6.2	Relative effect with respect to Sea Level Rise	30
6.3	Morphological impact	30
6.4	Conclusion	30
7	Discussion on maximum allowable head difference over the barrier	31
8	Summary	34

9 References	36
9.1 Reports used for this summary report	36
9.2 Additional references	36

1 Introduction

1.1 Background

The Eastern Scheldt Storm surge barrier was built to protect the south-western delta of the Netherlands against flooding while the marine environment of the Eastern Scheldt estuary is conserved as much as possible. The barrier was completed in 1986. The storm surge barrier has 62 gates, distributed over 3 barrier sections. The gates are open during normal conditions to allow the tide to enter the Eastern Scheldt and closed during severe storm surges.

The volume of, water entering the Eastern Scheldt Estuary each tide is less than before the construction of the barrier. This has affected the sediment transport and consequently the morphology of the estuary and resulted in a 'sand demand' of the system. The old tidal channels are basically too deep for the reduced tidal dynamics and tend to accrete. The sand for this originates from the tidal flats, which are eroding.



Figuur 1.1 Left: Eastern Scheldt Storm Surge Barrier during a storm and Right: tidal flow through the gates of the Eastern Scheldt Barrier during ebb (© Rijkswaterstaat).

In 2016 Rijkswaterstaat (RWS), the responsible agency of the Ministry of Infrastructure and Watermanagement, allocated two gates in the Roompot Section of the barrier (most southern section) for the recovery of tidal energy. Tocardo obtained permits to install tidal turbines in both Gate 8 and Gate 10. At the end of 2015, the first tidal power plant consisting of 5 tidal turbines was installed in Gate 8. Tocardo's preparations for a tidal power plant in Gate 10 are ongoing.

Since the tidal power plant can be considered as an extra obstruction to the flow through the barrier, RWS would like to know the environmental effects of this. The main concerns of RWS are the flow patterns around the tidal turbines and the potential effect of the tidal turbines on the bed protection.

1.2 Requirements of the permits

The permits contain requirements that limit the operation of the tidal power plant:

- Lifting of tidal power plant when the head difference over the barrier exceeds 80cm during flood;
- Lifting of tidal power plant when the head difference exceeds 60cm during ebb.

Furthermore, the permits require Tocardo to monitor the environmental impact of the tidal power plants. The following effects need to be assessed by Tocardo [6]:

- Effects on the flow through the barrier;
- Effects on the bed protection;
- Effects on the deformation of the barrier.

To investigate the potential effects on the flow through the barrier, including the potential effects of the turbines on the bed protection, several studies have been performed, see references [1] to [5]. This report describes the results of these studies. The results of the regular surveys of the bed protection and the deformation measurements of the barrier are reported elsewhere.

1.3 Objective and study subjects

The overall objective of this study is:

To assess the impact on the environment of the tidal power plant in Gate 8 of the Roompot Section of the Eastern Scheldt Storm Surge barrier.

The above objective is met by assessing the available measurements that have been performed prior and after installation of the tidal turbines. In combination with computer simulations, insight is given in the effects of the tidal turbines on the different environmental aspects, such as the discharge capacity of the gate in question, and the changes in flow patterns near the bed protection and the potential morphological changes. To assess the impact of the tidal power plant, several detailed studies have been conducted to analyse potential effects of the turbines on the following subject:

- 1 changes in tidal ranges in the Eastern Scheldt, by analysing long-term water level data,
- 2 the discharge capacity of the barrier by means of current measurements and detailed numerical simulations,
- 3 the large-scale flow patterns in the Roompot Section,
- 4 the local flow field especially near the bed protection,
- 5 the morphology in the Eastern Scheldt by investigating sedimentation and erosion processes of the intertidal areas.

The limitations of the present permit restrict the amount of energy that can be generated by the tidal power plant. Therefore, Tocardo wishes to increase the operational window to a maximum head difference of 90cm for both ebb and flood, provided that it can be shown that the safety of the barrier is not compromised. This wish applies to the existing pilot plant in Roompot Gate 8, and to the planned tidal power plant in Roompot Gate 10 as well. Chapter 7 of the report discusses the suitability of the present results to judge the feasibility of an increase of the operational head to 90 cm for ebb and flood.

1.4 Research frameworks

The study subjects presented above were investigated within the framework of 2 research projects: the Dutch Marine Energy Centre or DMEC project (Deltares project number 11200119) and the Oosterschelde Tidal Power or OTP project (Deltares project number 11200444). During the investigations close contact was maintained with the PhD candidate of the New Delta project of the TUDelft on tidal turbines in the Eastern Scheldt Barrier.

1.4.1 DMEC project

In the DMEC project a consortium of 15 partners investigated topics that are related to 'energy from water'. The DMEC project was carried out under the Program 'Opportunities for

West', ('Kansen voor West II'), and funded by the European Regional Development Fund (ERDF) and the Province of Noord-Holland. The relevant research subjects are part of the DMEC project - Work Package WP 3.7, which is led by Deltares. WP 3.7 aims to use and develop tools to investigate the near-field and far-field hydrodynamics due to the Tidal Power Plant in Gate 8 of the Eastern Scheldt Storm Surge barrier. Under this WP, the following subjects have been addressed (numbers refer to the subjects in Section 1.3):

Subject	Description	Remarks
2b	Creating a detailed numerical model of the flow around the tidal turbines	
4	Analysis of the effects on bed protection	M.Sc. Thesis project TUDelft
5	Large-scale morphological impact	M.Sc. Thesis - In cooperation with TUDelft – OTP project

Under 'remarks' it is indicated how the subjects are related to graduate projects and the OTP project at the TUDelft.

1.4.2 OTP project

In the OTP project a consortium of 6 partners investigated the effects of the tidal turbines on the environment. The OTP project was carried out under the 'Operational Program Southern Netherlands' (OPZuid), and funded by the European Regional Development Fund (ERDF) and the Province of Zeeland. This research is part of the OTP project - Work package 1, which is led by Deltares. WP 1 aims to investigate the environmental effects of the tidal turbines. Part of this WP is to investigate the effect of the tidal turbines on the changes in tidal range. Below a list is given of the subjects that have been investigated under the OTP project:

Subject	Description	Remarks
1	Effect on water levels by analysing changes in tidal range	Part of the monitoring plan [6]
2a	Analysing changes in flow patterns by analysing measurement data	In cooperation with TUDelft – New Delta project 869.15.008 and OTP project Part of the monitoring plan [6]
3	Changes in large-scale flow patterns	

Under 'remarks' the relation with the OTP monitoring plan and the PhD and OTP project at the TUDelft is shown.

1.4.3 NWO The New Delta project on tidal turbines in the Eastern Scheldt Barrier

The research project (number 869.15.008) addresses the flow interaction at semi open barriers with free stream turbines. It is part of the research programme The New Delta, which is financed by the Netherlands Organisation for Scientific Research (NWO). The study is performed by PhD candidate Merel Verbeek, and guided by Prof.Dr.Ir. W.S.J. Uijttewaal and Dr. Ir. R.J. Labeur of the TUDelft. Compared to the work reported here the New delta project has a more scientific approach and longer time horizon. Investigators on both sides profited of the close cooperation, particularly with respect to data acquisition and processing.

1.4.4 Project team

The subjects listed above were investigated in the different research projects in close consultation between the Tidal Power Plant developer and operator Tocardo, and researchers

of the TUDelft and Deltares. Below the key researchers of Deltares and the TUDelft are listed per subject:

Subject	Description	Key personnel
1	Effect on water levels by analysing changes in tidal range	Emiel Moerman
2a	Analysing changes in flow patterns by analysing measurement data	Wilbert Verbruggen, Merel Verbeek (TUDelft)
2b	Creating a detailed numerical model of the flow around the tidal turbines	Tom O'Mahoney
3	Changes in large-scale flow patterns	Remco Plieger, Anton de Fockert
4	Analysis of the effects on bed protection	Thieu Stevens, Anton de Fockert, Tom O'Mahoney
5	Large-scale morphological impact	Kamilla Guijt, Arnout Bijlsma, Marco Gatto (TUDelft)
	Senior adviser	Arnout Bijlsma
	Project management	Anton de Fockert

2 Subject 1: Effect on water levels

A detailed analysis has been made of water level measurements in- and outside of the Eastern Scheldt, and with and without the presence of the tidal turbines. The details of this analysis are described in [1]. In this Chapter, a brief description of the approach and the results are presented.

2.1 Approach

In the assessment, two types of analyses have been carried out. First, a regression analysis has been performed on the tidal ranges (i.e. the vertical difference between consecutive high and low waters) of the tidal stations *Roompot Binnen* and *Roompot Buiten*. These stations are located respectively inside and outside the barrier just north of the Roompot Section. Secondly, an analysis has been made in which the tidal range is shown against the natural variation due to the 18.6 year lunar tidal cycle.

2.2 Regression analysis tidal range Roompot Binnen and Roompot Buiten

In 2014, a study has been conducted to determine the linear regression between the tidal ranges of *Roompot Buiten* and *Roompot Binnen*. For individual years and relevant periods a (first-order, $y = ax + b$) linear fit between the tidal ranges of the two stations was made. From this analysis the variation in the annual mean tidal range over the years was assessed. This assessment has been extended (see [1]) with the years 2014, 2015 (before installation) and one year in which the array of tidal turbines has been in operation (June 2016 - May 2017¹). It is relevant to note that in this period the turbine operation was restricted by (i) maximum head restrictions of 0.6 and 0.8 m for ebb and flood, respectively, and (ii) maintenance and modifications. Overall, the turbines were in the water for nearly 50% of the time.

The assessment showed that for the period with turbine deployment, the mean tidal range at Roompot Binnen derived from the annual regression analysis for a given mean tidal range at Roompot Buiten of $x = 285$ cm is about 2cm lower than for the years prior to turbine deployment [1]. The ~2 cm can be significant since they exceed the range of 2 standard deviations (~1.4 cm) below the mean value of the years before 2016. On the otherhand, when comparing within the period of June 2016 - May 2017 the mean tidal ranges at Roompot Binnen derived from regression analysis of the data labelled turbines 'operational' and turbines 'parked', no significant differences were found. This means that based on 1 year of measurements after turbine installation, no clear effect of the tidal turbines on the water levels in the Eastern Scheldt could be detected.

2.3 Long-term variation

To analyse the long-term variation in tidal range, the data have been analysed based on annual mean tidal range per station. In the long-term data a clear variation was observed representing the 18.6 year tidal cycle, see Figure 2.1, where the station of Westkapelle illustrates the long-term variation since 1880, well before the start of the Delta Works. The analysed operational period (1 June 2016 to 31 May 2017) falls within the observed descending part of the cycle. The mean annual values therefore seem to fit within the natural cycle (see Figure 2.1). The Figure furthermore shows that the variation of the annual mean

¹ At the time of writing validated measurements of Roompot Binnen were lacking to add a second year (June 2017 – May 2018) to the analysis.

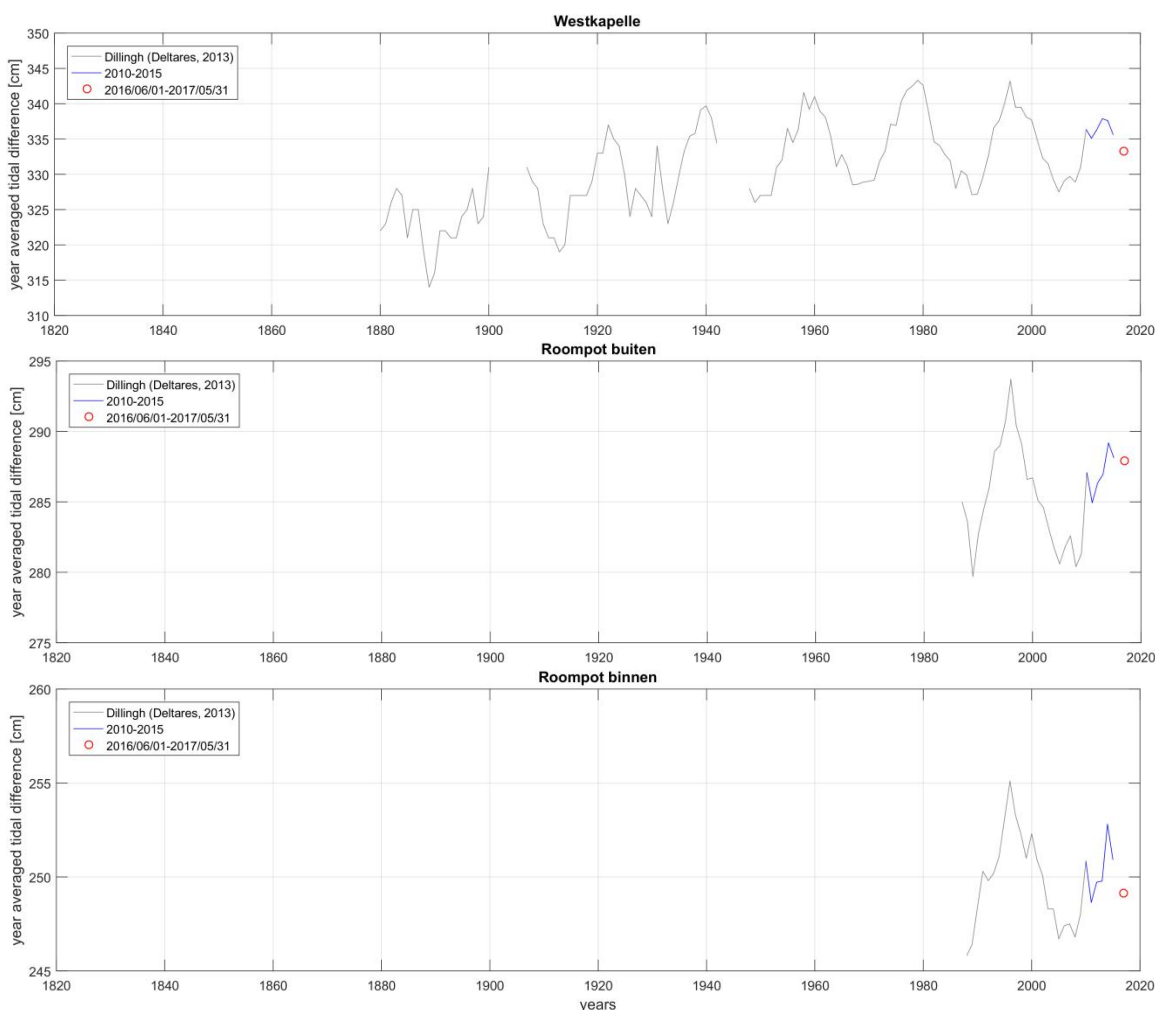


Figure 2.1 Annual mean tidal range until turbine deployment (grey and blue line) and after turbine deployment (red markers) for the water level measurement stations of Westkapelle, Roompot Binnen and Roompot Buiten.

tidal range is about 14 cm at Roompot Buiten and about 9 cm at Roompot Binnen (roughly 4-5% of the mean tidal range).

Focussing on the *Roompot Buiten* and *Roompot Binnen* stations, in Figure 2.2 the annual mean tidal ranges are presented again together with their relative difference (red line), i.e. the difference relative to the mean difference. From this it follows that the relative variation between the annual mean tidal range for *Roompot Buiten* en *Roompot Binnen* ranges from -3 cm to +3 cm. The result of the operational period is just within this range.

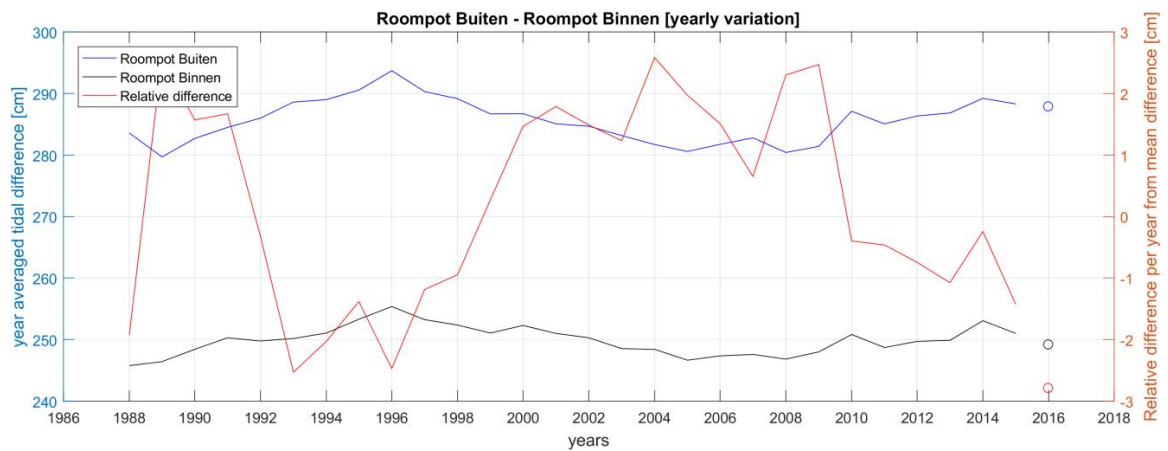


Figure 2.2 Variation of annual mean tidal ranges at Roompot Buiten and Roompot Binnen and their relative difference.

2.4 Conclusion

From the analysis of the water level measurements in the Eastern Scheldt, including one year of turbine operation, no clear effect of the tidal turbines on the tidal range in the Eastern Scheldt could be detected. To improve the analysis, longer series of water level measurements with turbine operation would be required. However, the effect of the tidal turbines will be significantly lower than the natural variation of the water levels, due to for instance the 18.6 year tidal cycle, storm surge frequency and barrier operation or long-term effects of the Eastern Scheldt Barrier construction and related morphological developments.

3 Subject 2: Effect on discharge capacity of the barrier

In this Chapter the effect of the turbines on the discharge capacity of the barrier is described. First, an assessment is presented based on the available current measurements. Because no firm conclusion could be drawn from these measurements, a detailed numerical flow model (CFD model) is used to assess the potential changes in discharge capacity. The analysis of the measurements is described in detail in [2] and the CFD model including validation is described in detail in [3]. This Chapter presents the main conclusions of both assessments.

To increase the understanding of the flow distribution in a Gate of the Eastern Scheldt Barrier, average flow profiles were analysed for selected head differences. These cases were selected on the basis of the available quality checked data for both the situation with and without turbine deployment. The selected cases are listed in Table 3.1.

Table 3.1 Selected conditions for the analyses.

	Case number	Water Level North Sea	Water Level Eastern Scheldt	Head difference
		[m; NAP]	[m; NAP]	[m]
Ebb	1	0.93	1.13	-0.20
	2	0.68	1.00	-0.32
Flood	3	-0.57	-0.77	0.20
	4	1.12	0.57	0.55

3.1 Subject 2A: Analysis of current measurements

3.1.1 Measurement setup

To assess the flow through the Eastern Scheldt Storm Surge Barrier ADCP measurements have been performed. In 2011, ADCP measurements have been carried out in Gate 8 of the Roompot Section of the Eastern Scheldt barrier. This measurement campaign consisted of 2 Teledyne RDI ADCP's, which were measuring in horizontal and vertical direction. The vertical ADCP was mounted on the inner side of the sill (estuary side) and the horizontal ADCP was mounted on Pillar 9 (see Figure 3.1). Due to the distance between the 2 ADCP's the measurement cells were not overlapping. The measurements were carried out for a period of 6 days.

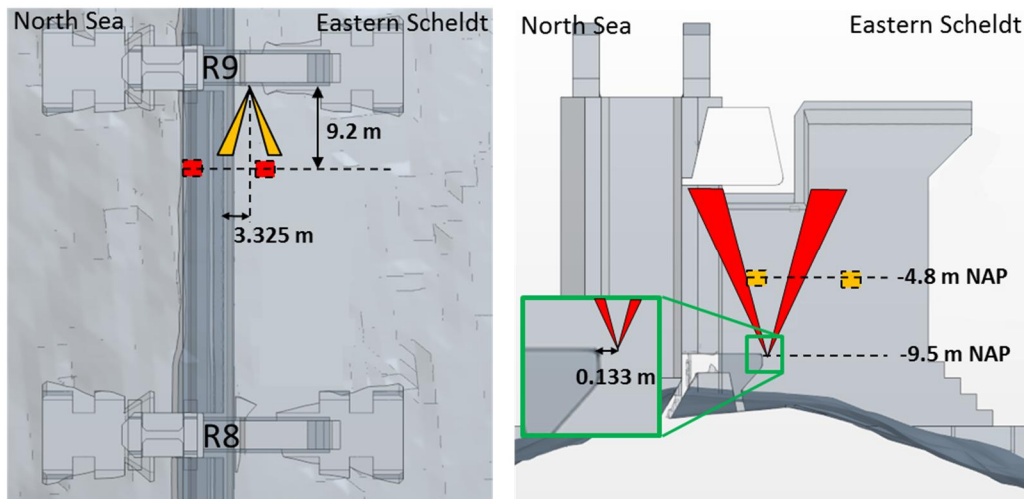


Figure 3.1 Overview of the 2011 ADCP measurements. Left: Top view, right: Side view.

In 2015, 5 turbines were installed on the Eastern Scheldt side of Gate 8 of the Roompot Section. The middle and outer turbines were equipped with two Nortek ADCP's, one pointing forward (towards the North Sea) and one pointing backward (towards the estuary), see Figure 3.2. The forward looking ADCP was mounted on the strut of the turbine and the backward ADCP was located in the rear of the nacelle. The ADCP devices measure along the central beam by default (in main flow direction), but have also been used to perform 5-beam measurements. On request measurements with different configurations have been carried out, see Table 3.2.

Table 3.2 ADCP measurement periods with and without turbines.

Measuring period		Turbine operation	Signal
15/08/2011 – 21/08/2011	6 days	No turbines	Horizontal + vertical ADCP
10/10/2016 – 26/10/2016	14 days	Normal operation	1 beam
22/06/2017 – 24/06/2017	1 day	Normal operation	5 beams
28/08/2017 – 29/08/2017	1 day	Stall mode	1 beam
14/09/2017 – 15/09/2017	1,5 day	Stall mode	5 beams

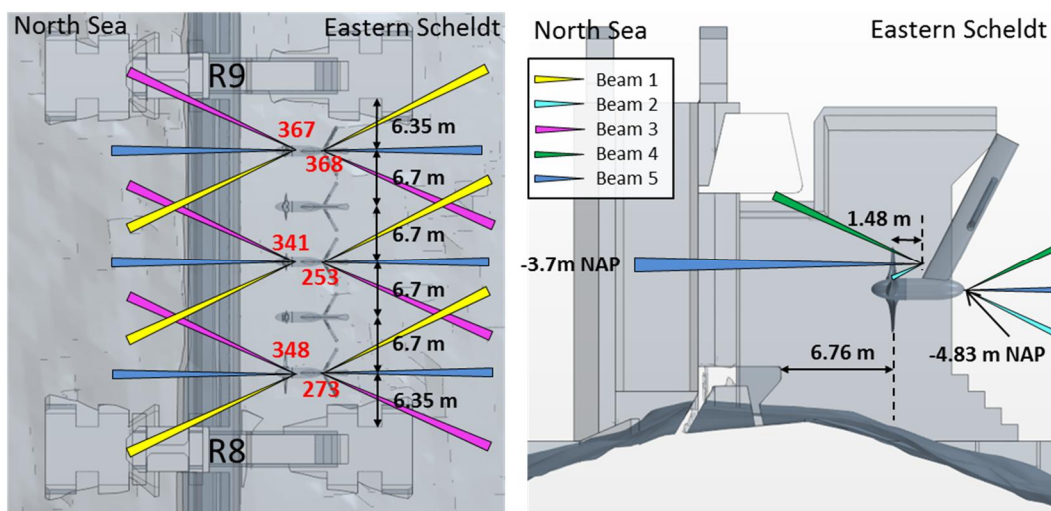


Figure 3.2 Top view (left) and side view (right) of the turbine configuration at Gate 8 of the Roompot Section. The red numbers show the names of the forward-looking and backward-looking ADCP devices.

3.1.2 Analysis

A general comparison has been made between the situation with and without turbines. The vertical velocity profile for the ebb case with a head difference of 20cm is presented in Figure 3.3. In Figure 3.4, the horizontal velocities are presented for the situation with turbines during ebb. In this figure it is seen that the standard deviation of the velocities in the wake of the turbine are much larger than upstream of the turbine. In both situations, higher velocities are measured at the end of the tidal phase than at the start of the tidal phase (blue lines give higher velocities than black lines in Figure 3.3 and Figure 3.4). This difference is caused by the inertia of the tidal flow.

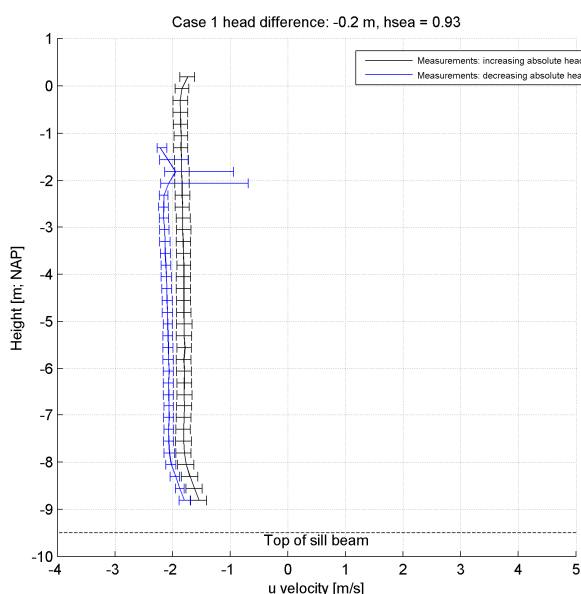


Figure 3.3 Velocity measurements of the vertical ADCP at the sill for a head difference of 20cm during ebb without turbines.

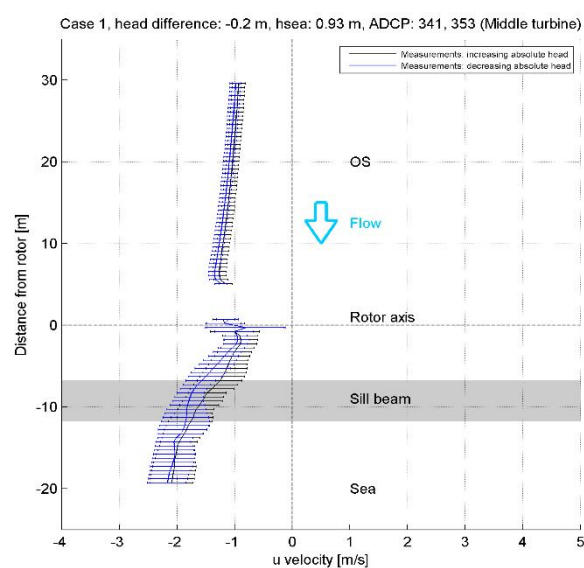


Figure 3.4 Horizontal velocity measurements of the ADCP's mounted on the turbine for a head difference of 20cm during ebb with turbines.

Apart from the measurement orientation and location the instruments, the spatial resolutions (bin size) and sampling rates differ between surveys for the situation with and without turbines. All of this introduces uncertainty and therefore it is difficult to compare the measurements. The best position to compare the velocities from the ADCP measurements is at the height of the axis of the turbines (NAP -4.8m). The results of this comparison is presented in Figure 3.5. In this graph, a comparison is made for different head differences against the velocity. It should be noted that only during flood an undisturbed velocity profile could be measured. During ebb, the horizontal velocity is measured in the wake of the turbine. Because of this, the velocity variation is much larger in the wake.

Figure 3.5 shows that the velocity during flood is about 5-10% higher for the situation with turbines than for the situation without turbines. This is counterintuitive. However, considering the standard deviation of the measurements, and the uncertainty arising from ADCP orientation, configuration and type, and (especially) measurement location, 5% difference seems reasonable and any effects from the turbines negligible.

To avoid the drawbacks of the previous comparison, a one day measurement campaign has been held with the turbines in stall mode. In this situation, the turbines rotate at a very low speed (< 4 RPM) and extract very little energy. This results in a strong reduction of the

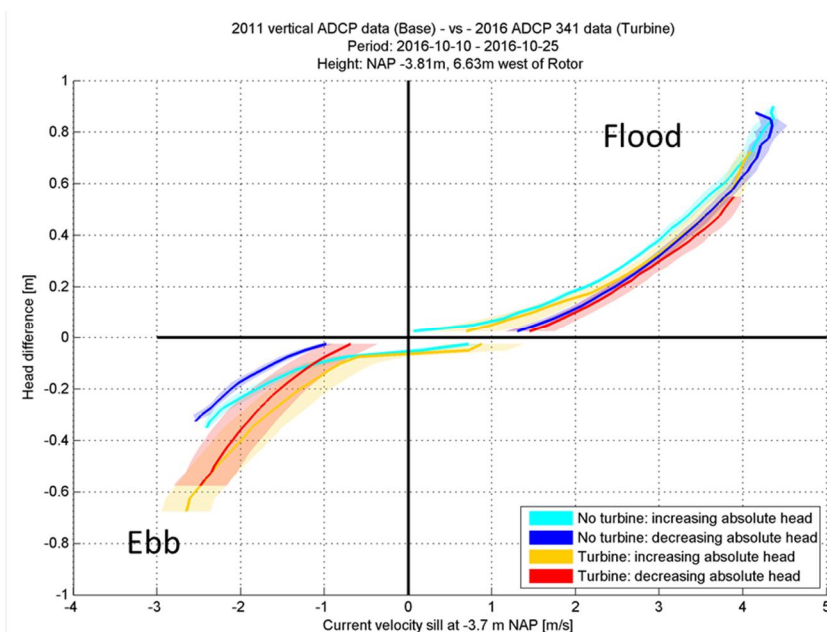


Figure 3.5 Comparison of the 2011 vertical ADCP data (No Turbine) and the 2016 forward-looking ADCP data (Turbine) at the overlapping location versus the head difference. The lines show the median values and the patches show the bandwidth of the data (\pm one standard deviation). For the period during turbine deployment, the forward-looking ADCP of the middle turbine is used (ADCP 341).

resistance to the flow and can be considered very close to a condition in which the turbines do not exist, while the measurement setup remains the same. The general observation is that for ebb flow (Figure 3.6) no differences in upstream flow are observed, while downstream of the turbine, in the turbine wake, the flow velocities are much larger during stall mode (red/pink line) than for normal operation (blue/black lines). The figure suggests that the wake has probably recovered by roughly 30 m downstream of the rotor.

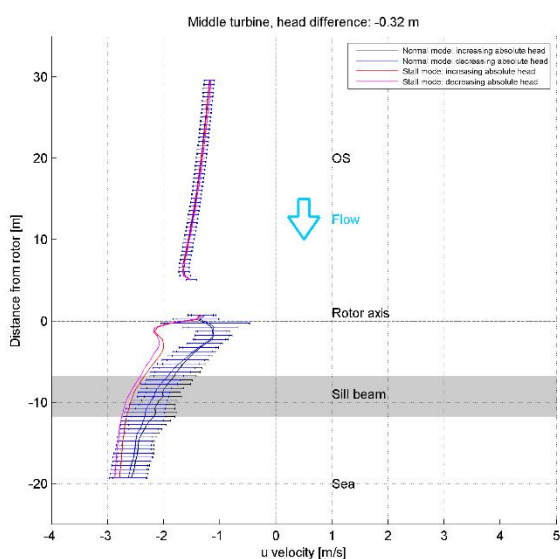


Figure 3.6 Velocity profile for Case 2 (head difference of -0.32 m) as measured by the forward-looking and backward-looking ADCP devices on the middle turbine for both normal and stall mode.

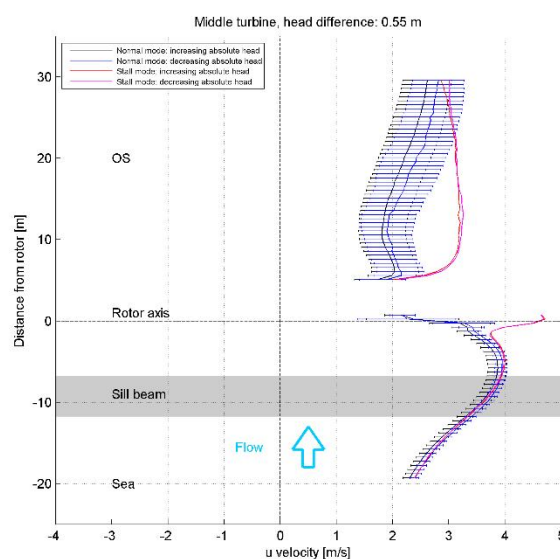


Figure 3.7 Velocity profile for Case 4 (head difference of $+0.55$ m) as measured by the forward-looking and backward-looking ADCP devices on the middle turbine for both normal and stall mode.

During flood no clear distinction is observed above the sill between the situation with turbines in stall mode compared to the situation with normal operating turbines (see Figure 3.7). Similar to ebb, the velocity profile downstream of the turbines is different, due to the strongly reduced wake for the situation of stall mode. The figure shows that the wake has largely recovered by about 30 m downstream of the rotor.

Additionally, a comparison has been made between the 5 beam ADCP data in stall mode and in normal mode. The forward looking ADCP's on turbine 1 and turbine 5 did not work, and therefore the comparison for these turbines is lacking. Figure 3.8 and Figure 3.9 present the differences in flow velocities in beam direction between stall mode and normal mode for respectively flood and ebb. At the downstream side of the turbines a clear acceleration is observed in-between the turbines during flood. It is also seen that flow is bypassing the turbines between the turbines and the pillars. Upstream of the turbines practically no change in flow velocities is observed both during flood and ebb, except close to the rotor plane.

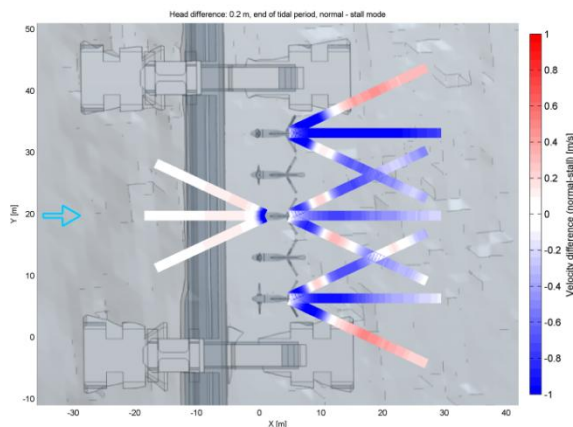


Figure 3.8 Comparison of the measured velocities along 5-beams during normal operation against stall mode operation for Case 3 (flood).

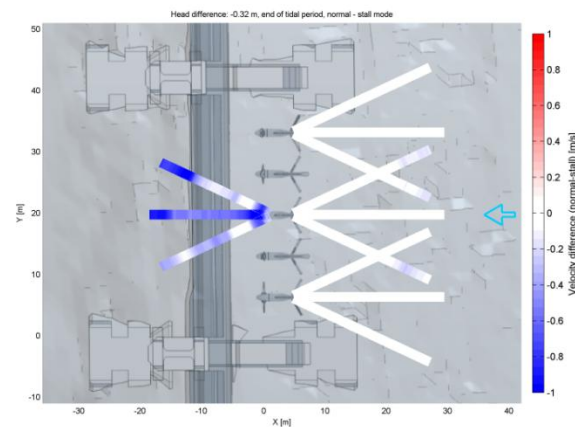


Figure 3.9 Comparison of the measured velocities along 5-beams during normal operation against stall mode operation for Case 2 (ebb).

3.1.3 Discharge coefficient

Based on the measured velocities, an estimate was made of the discharge coefficient through the barrier for the situation with and without turbine deployment. Due to the inertia, two different average velocities were measured for one value of the head difference, and two different discharge coefficients were obtained. By incorporating the uncertainty of the velocity measurements, the uncertainty range in the discharge coefficient increased to 5-10%. This range is too large to obtain a reliable estimate of the change in discharge coefficient due to the deployment of the tidal turbines.

3.1.4 Conclusions

Different ADCP measurements have been carried out prior to the installation of the tidal turbines and after deployment. The use of the current measurements to assess the change in discharge coefficient due to the tidal turbines during flood did not provide reliable results due to the lack of overlap in measurement cells and the large uncertainty in the measurements. During ebb, the Gate opening is in the wake of the tidal turbines, which increases the inaccuracy of the discharge estimate significantly.

Note that no change in the upstream flow was observed from a comparison of measurements when the turbine was operational and when in stall mode, effectively a non-operational condition.

Though no reliable estimate of the effect of the turbines on the discharge coefficient could be derived from the current measurements, these measurements were very useful to validate the detailed numerical model, see Section 3.2.

3.2 Subject 2B: CFD simulations

Because the current measurements could not give a reliable estimate of the effect of the tidal turbines on the discharge coefficient, the CFD model setup in the DMEC project was used for an alternative approach. This section describes the CFD model used to assess the flow through the barrier and the tidal turbines and subsequently the assessment of the change in discharge coefficient.

The details of the CFD model are described in [3]. This section only describes briefly the setup and the results of the modelling.

3.2.1 Characteristics of the CFD model

A CFD model has been setup for a section of the storm surge barrier using the StarCCM+ software package. Two model versions are available: one of the storm surge barrier without tidal turbines and one including the tidal turbines. The model has a length of approximately 400m (200m at both sides of the barrier) and consists of Gate 8 plus the two half Gates of 7 and 9. The bathymetry is derived from multibeam surveys by Rijkswaterstaat (see Figure 3.10). The resolution of the survey needed to be reduced from 0.5 m to 2 m.

For both the situation with and without turbines, the operational cases as defined in Table 3.1 are simulated by the numerical model.



Figure 3.10 Contour plot of the bed elevation. Dimensions are with reference to NAP.

For the simulations with turbines, the turbines have been included in the domain together with their support structures (see Figure 3.11). The turbines have the ability to rotate in the model by the correct rotational speed of the turbines. The models run in transient mode for a simulation period of 10-20 minutes.

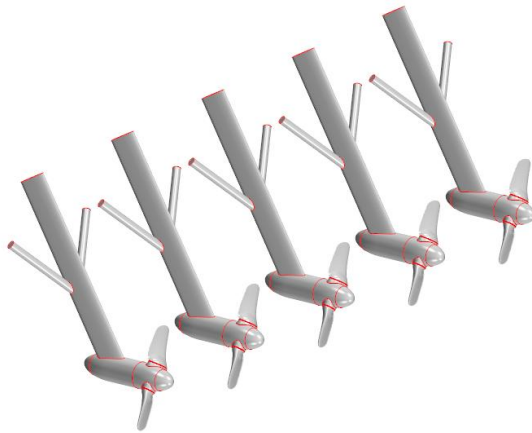


Figure 3.11 3D CAD view of the five turbines with support structure.

The computational mesh has been generated in Star-CCM+ using multiple areas of mesh refinement (see Figure 3.12). The largest cells in the domain are located in the far-field near the boundaries (cube cells of 1.2 m) and the smallest cells are located in the gate and around the sill (16cm). Near the bed and along the walls of the barrier structure, a resolution of 3mm is used. In the cases where the turbines are included, the mesh in the turbine wake region is refined to 32 cm and the rotating zone around the turbine is further refined to 8 cm and even more refinement is added at the turbine itself in order to better model the boundary layers (see Figure 3.13). The mesh around the turbine blades rotates during the simulation.

Multiphase flow simulations are set up, modelling the air-water phases and the water surface. To model turbulence near the turbines and near the sill of the barrier, the Improved Delayed Detached Eddy Simulation (IDDES) turbulence model has been applied. This model uses a Large-Eddy Simulation approach in the bulk of the flow and a Reynolds-Averaged Navier Stokes approach in the near wall region.

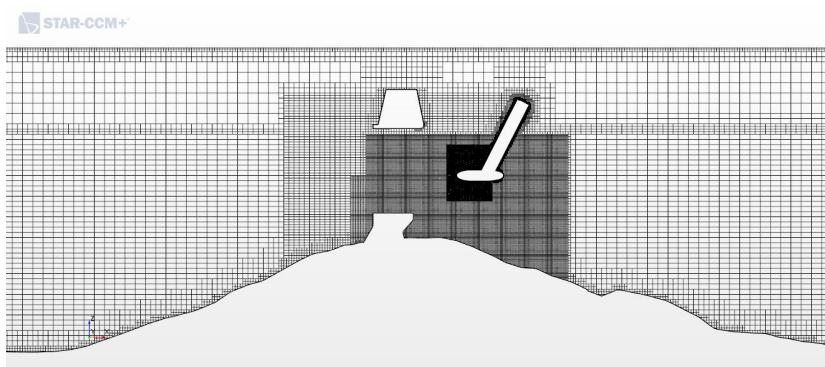


Figure 3.12 Detail of the mesh refinement zones around the sill of the barrier.

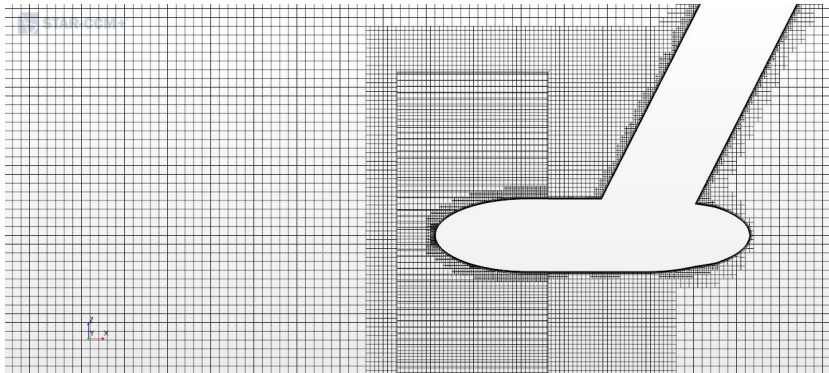


Figure 3.13 Detail of the mesh refinement zone around the turbine.

The model is forced by means of a velocity profile upstream, which is representative for the undisturbed velocity profile at 200m from the barrier. Similar to the real operation, the turbine rotation is applied to the model as a boundary condition. The rotational speed for each of the turbines was provided by Tocardo.

3.2.2 Model validation

Both CFD models have been validated based on the ADCP velocity measurements as described in Section 3.1. Figure 3.14 shows the velocity profile for (Ebb) Case 2 without turbines (NT.2) averaged over the 15 minutes (top) and an instantaneous velocity profile (lower plot). From this figure, the flow detachment at the sill is clearly visible. The highest velocities are observed at the water surface and a recirculation flow is present at the bed behind the sill. The flow pattern for flood is fairly similar.

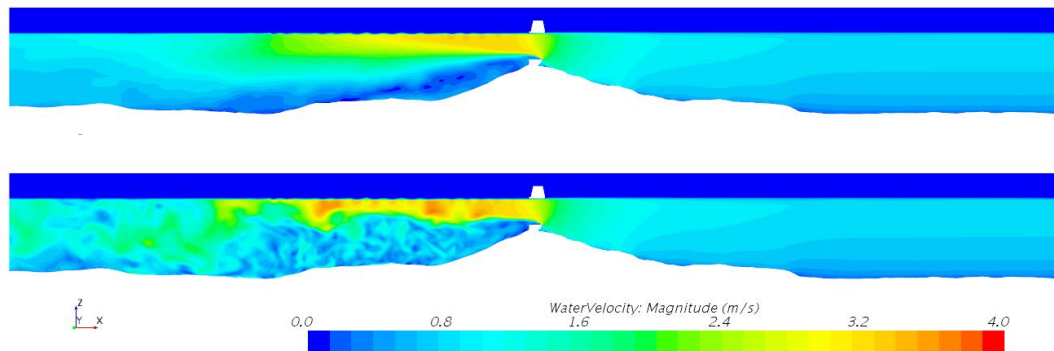


Figure 3.14 Contour plot of velocity magnitude on a vertical cross section from case NT.2; an ebb case. Top: average velocity field, bottom: instantaneous velocity field.

In Figure 3.15, the comparison of the simulation result against the vertical ADCP measurement is presented for (Ebb) Case 1 without turbines (NT.1). Because the CFD model is forced with steady boundary conditions, the effect of inertia is not present in the model. From this figure, it is concluded that the CFD results matches well with measured velocities.

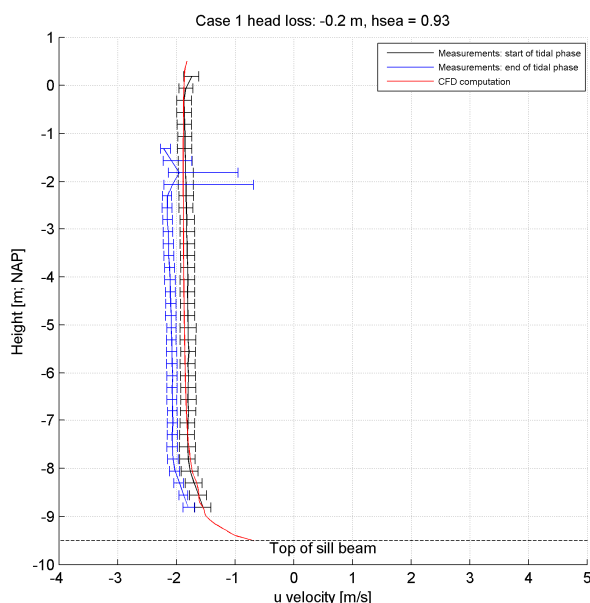


Figure 3.15 Vertical ADCP profile from the measurements without turbines – comparison between CFD and measurements – Ebb Case NT.1.

A similar validation has been performed for the situation with turbines. In these cases not only the velocity profiles are validated, but also the power and thrust as monitored on the turbines. In Figure 3.16, the mean velocity around the tidal turbines is presented in the top figure and an instantaneous velocity field is presented in the lower plot for (Flood) Case 4, with turbines (WT.4). In this figure, the energy extraction by the turbines is clearly seen in the lower velocity behind the turbines. Just below the turbines, a narrow acceleration zone is present. This is explained in more detail in [3].

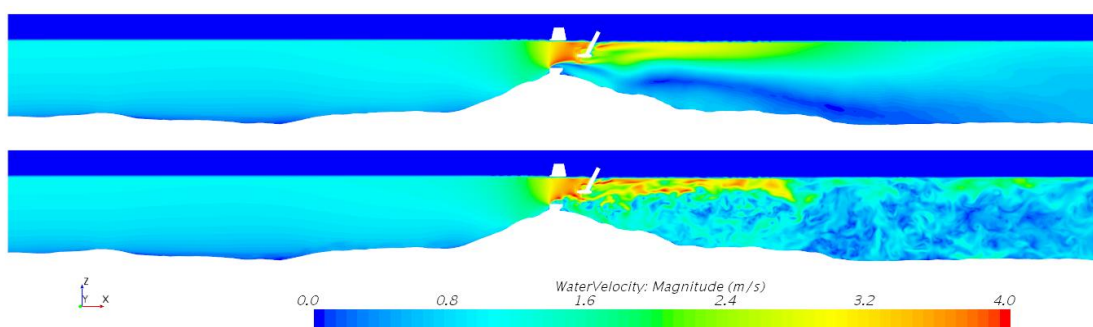


Figure 3.16 Contour plot of velocity magnitude on a vertical cross section from case WT.4; a flood case. Top: average velocity field, bottom: instantaneous velocity field.

In Figure 3.17, the results of the CFD model for the (Ebb) case with turbines (WT.1) are presented against the measured results from Section 3.1. For clarity, the model results for the same situation without turbines is also presented in this graph (NT.1).

From this figure, it is seen that upstream of the tidal turbines, the CFD model slightly under predicts the measurements. This is consistent with the earlier observation in Section 3.1.2 that the ADCP of the turbine measured about 5% higher velocities during flood compared to the vertical ADCP measurement without turbines. Downstream of the turbine, the CFD model

results fit within the velocity bandwidth of the wake of the turbine. The comparison between the CFD model results with and without turbines show that the velocities for the case with turbines is somewhat lower. This is caused by the blockage induced by the turbines. Therefore, a smaller discharge flows through the gate for a similar head difference.

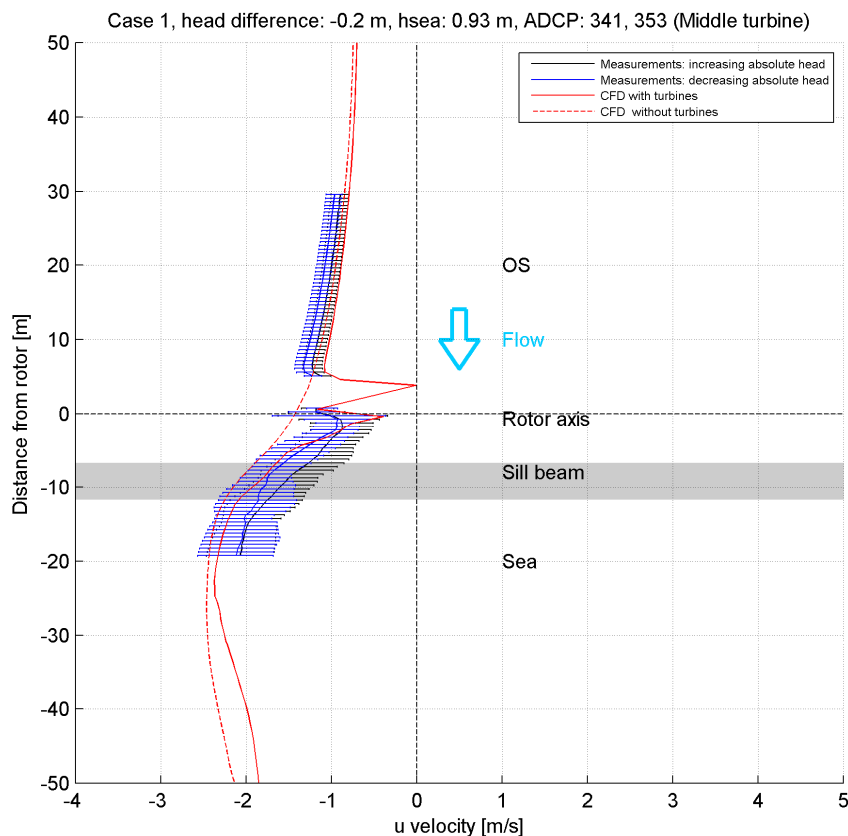


Figure 3.17 Longitudinal ADCP profile from the measurements with turbines – comparison between CFD and measurements – Ebb Case WT. 1. For illustrative purposes, the profile along the same line is also plotted for the corresponding simulation without turbines NT. 1.

Next step in the validation of the model is the comparison of the measured power and thrust against the modelled power and thrust. The power is not obtained directly from the simulations, but computed via the formula: $P = \tau\omega$, in which τ is the torque [Nm] and ω is the angular velocity [rad/s].

It was found that the model represents the measured power well. The deviation between the modelled power and measured power is approximately 10%, with a standard deviation in the modelled power of 5-10% and a standard deviation in the measured power of 10-20%.

The measured thrust was compared for the 2 turbines where thrust measurements have been performed. From this analysis follows that the standard deviation of the modelled thrust is about 5% and the standard deviation of the measured thrust ranges from 10-30%. The deviation between the modelled thrust and measured thrust is approximately 5%. Therefore, it is concluded that the model represents the thrust sufficiently accurate.

3.2.3 Discharge coefficient

The CFD model has been used to estimate the discharge coefficient through the barrier. For all cases, a comparison is made between the computed discharge coefficient for a gate with turbines and a gate without turbines by comparing the discharge through gate with turbines to the discharge through the neighbouring half gates. The result is that the discharge coefficient decreases by approximately 5% for ebb, while the discharge coefficient for flood does not change (see Table 3.3).

Table 3.3 Discharge coefficient derived from the CFD model results.

	Case	Head [m]	Discharge coefficient (μ)		Δ %
			without turbines [-]	with turbines [-]	
Ebb	1	-0.19	0.97	0.93	5%
	2	-0.32	0.98	0.92	6%
Flood	3	0.21	0.85	0.85	0%
	4	0.54	0.88	0.88	0%

3.3 Conclusions

Prior to the installation of the tidal turbines, current measurements were performed of the flow through the barrier. After deployment of the turbines a new set of current measurements was obtained. However, it turned out that these measurements could not be used to provide a sufficiently reliable estimate of the impact of the tidal power plant on the discharge through Gate Roompot 8 of the Eastern Scheldt Barrier.

In an alternative approach detailed CFD models were used, which were validated against the available velocity measurements, and the power and the thrust measurements.

Based on the validated CFD model more reliable estimates could be made of the changes in discharge capacity due to the presence of the tidal turbines. It was concluded that the discharge capacity of Gate Roompot 8 hardly changes during flood and decreases by about 5% during ebb. The main reason for this is the fact that the turbines are positioned upstream of the barrier sill during ebb and sufficiently far downstream of the barrier sill during flood. During ebb, the turbines are blocking the flow towards the barrier, while during flood the influence of the turbines on the flow becomes effective after the flow has passed the narrowest cross section of the gate (above the sill).

4 Subject 3: Changes in large-scale flow patterns

The effect of the tidal turbines on the discharge capacity of Gate Roompot 8 of the barrier is described in Chapter 3. To estimate the large-scale effect of a reduction in discharge capacity by tidal turbines the detailed ScalOost WAQUA model is used. This is a depth-averaged operational tide and storm surge model for the Eastern Scheldt Estuary and outer delta. It was developed by Deltares for Rijkswaterstaat. The details of this model are described in [7].

Apart of Gate Roompot 8, Tocardo has a permit to install tidal turbines in Gate Roompot 10 as well. Therefore, the impact of this tidal power plant has also been included in the model simulations. Since the design of the tidal turbines in Gate 10 is not yet available, an estimate had to be made on the change in discharge coefficients for this particular case. In consultation with Tocardo, it was decided to use the modified discharge coefficients as derived by Deltares in 2010 [8] for Gate 8. These discharge coefficients are much more conservative than the discharge coefficients derived in Chapter 3 for the tidal turbines in Gate 8 (see Table 4.1).

Table 4.1 Multiplication factors for the discharge coefficients to implement the tidal turbines in the WAQUA-ScalOost model.

	Opening	
	# 8	# 10
Ebb	0.95	0.923
Flood	1.00	0.875
Sill height (w.r.t. NAP)	-9.5	-10.5

In the WAQUA model, the discharge coefficient is used to define an energy sink in the model in combination with the (wet) cross section of the gate. Because the sill height of Gate 10 is lower than of Gate 8, even more energy is dissipated in the model due to the tidal turbines in Gate 10 than in Gate 8.

4.1 Brief model description

Simulations have been carried out with the WAQUA ScalOost model version 5. From this numerical model, Case 046 is used as a reference. This case has been calibrated and has a very high accuracy with respect to the reproduction of the water levels in the Eastern Scheldt basin, see [7]. The water level deviation between the measurements and the modelling results for all measuring stations is maximum 5cm for the month of April 2007 (see Table 4.2).

Table 4.2 Accuracy of the WAQUA model for the month of April 2007 (obtained from [7]).

Simulation : OS046	Bias [m]	RMSE [m]	Std [m]	difMAX [m]	difMIN [m]
Haringvliet 10	-0.012	0.028	0.025	0.006	0.022
Brouwershavensche O	-0.039	0.053	0.035	-0.026	-0.002
OS14	-0.034	0.042	0.026	0.026	-0.008
OS11	-0.021	0.039	0.032	-0.054	0.029
OS4	-0.001	0.023	0.022	0.054	-0.006
Roompot Buiten	-0.003	0.026	0.026	0.073	-0.016
Roompot Binnen	0.011	0.050	0.048	0.006	-0.023
Stavenisse	0.007	0.027	0.026	-0.033	0.010
Krammersluizen Laag	-0.003	0.044	0.044	0.104	0.018
Yerseke	0.000	0.024	0.024	-0.054	0.041
Bergsediepsluis West	-0.006	0.031	0.031	-0.041	0.029
Marollegat	0.000	0.031	0.031	-0.055	0.055
Gemiddeld	-0.008	0.035	0.031	0.000	0.012

The ScalOost model has a resolution of one grid cell per gate opening or 45m at the barrier, which increases to about 100m at the edge of the bed protection. The domain of the ScalOost model is shown in Figure 4.1.

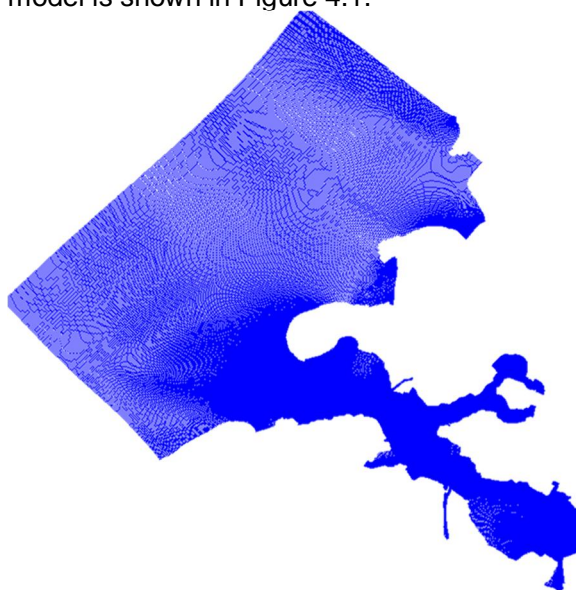


Figure 4.1 Model grid of the ScalOost model.

Time varying wind fields from the weather station “Vlakte van Raan” are included in the model. The model has been run for one year, with a specific focus on a detailed spring neap tidal cycle in July. In total, 3 simulations have been run:

- 1 Simulation without the presence of tidal turbines
- 2 Simulation with the presence of tidal turbines in Gate Roompot 8
- 3 Simulation with the presence of tidal turbines in Gates Roompot 8 and 10.

By comparing these results, the relative influence of the tidal turbines could be assessed.

The multiplication factors listed in Table 4.1 are imposed on the model. This means that different discharge coefficients are used for ebb and for flood to parameterize the tidal turbines. However, the operational regime of e.g. 60cm during ebb and 80cm during flood is not included in the model, because a time dependent change in discharge coefficient is not facilitated by the

WAQUA model. This means that in the simulations, the tidal turbines are always present. In the analysis below only the results occurring within the operational window of 90 cm head difference are considered.

4.2 Flow fields

Due to the additional resistance at Gates Roompot 8 and 10 in the cases with turbines, the total discharge through the barrier is slightly reduced. In Table 4.3, the change in the total discharge through the Roompot Section of the barrier is presented for the different simulations. From this table it is seen that the flow through this section reduces by about 1% due to the presence of the tidal turbines. Figure 4.2 shows the changes in discharge through the first 13 openings of the barrier. From this figure it is seen that the discharge is reduced through Gate 8 and 10 when the turbines are in operation, while in the adjacent gates no appreciable increase of the discharge is observed. Though this would agree with the observation that the upstream velocities do not change due to the turbines (Section 3.1.4), it remains to be seen if this is entirely correct. The flow bypassing will be addressed in more detail the New Delta project, mentioned in Section 1.4.3.

Table 4.3 Change in discharge through the Roompot section of the barrier by implementation of the tidal turbines.

Simulation		Change in discharge through Roompot	
		Ebb	Flood
1	No turbines	-	-
2	Turbines in R8	-0.4%	-
3	Turbines in R8&10	-1.0%	-1.0%

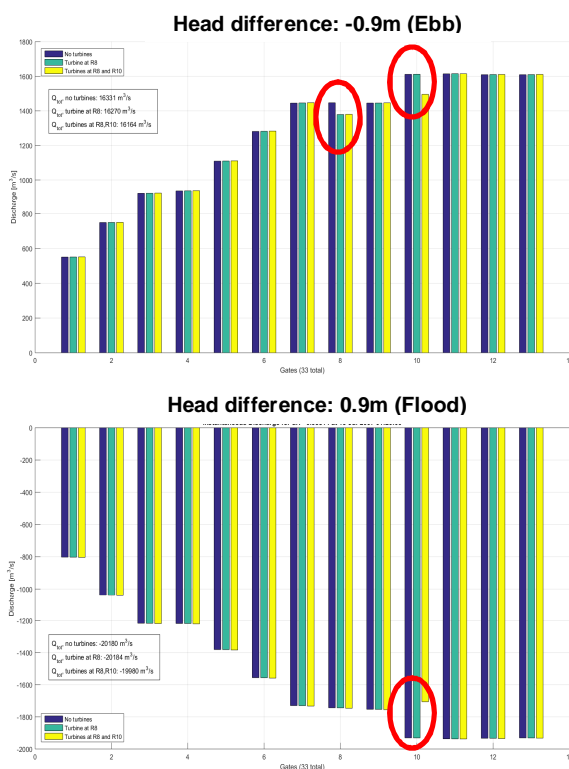


Figure 4.2 Flow through gate 1-13 of the Roompot section for the 3 simulated cases. The red circles indicate the presence of the tidal turbines in the model.

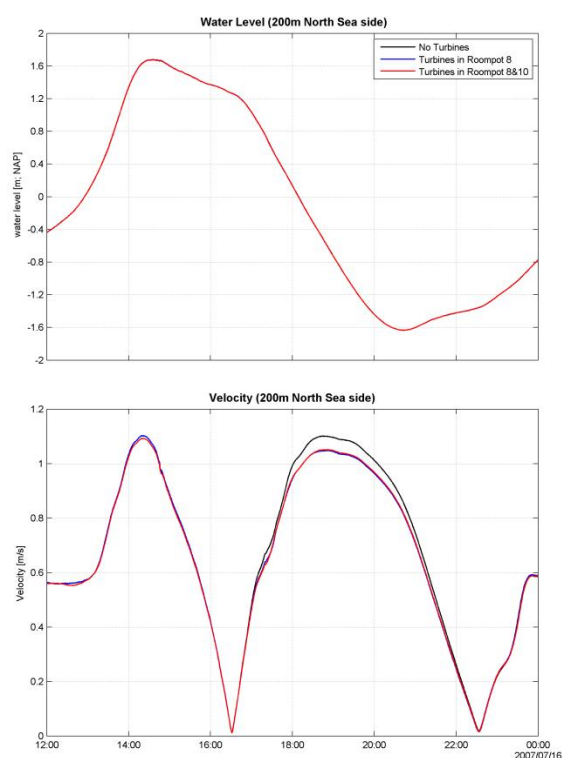


Figure 4.3 Water level and velocities at 200m from Gate Roompot 8 at the North Sea side for all simulated cases.

In Figure 4.3, the changes in velocities are shown at 200m from Gate Roompot 8 of the barrier at the North Sea side. In this simulation, a reduced velocity is observed for the situation with turbines during ebb. However, during flood, the change in velocity is negligible.

The changes in the velocity field due the presence of the tidal turbines in Gates Roompot 8 and 10 are observed along the whole Roompot section. Figure 4.4 shows the differences in velocity magnitude for a representative moment during neap tide. The full tidal cycle can be inspected in the animation that is provided in addition to this report. The maximum difference in velocity magnitude between the situation with turbines in Roompot 8 and 10 with the situation without turbines is about 10cm/s. The maximum difference in velocity magnitude between tidal turbines in Roompot 8 and the base situation is about 3cm/s. For this case, the changes are mainly found at the North Sea side during ebb. The largest changes in flow velocity are found behind the turbines and near the 'buitenhaven' (northern edge of the Roompot section on the North Sea side).

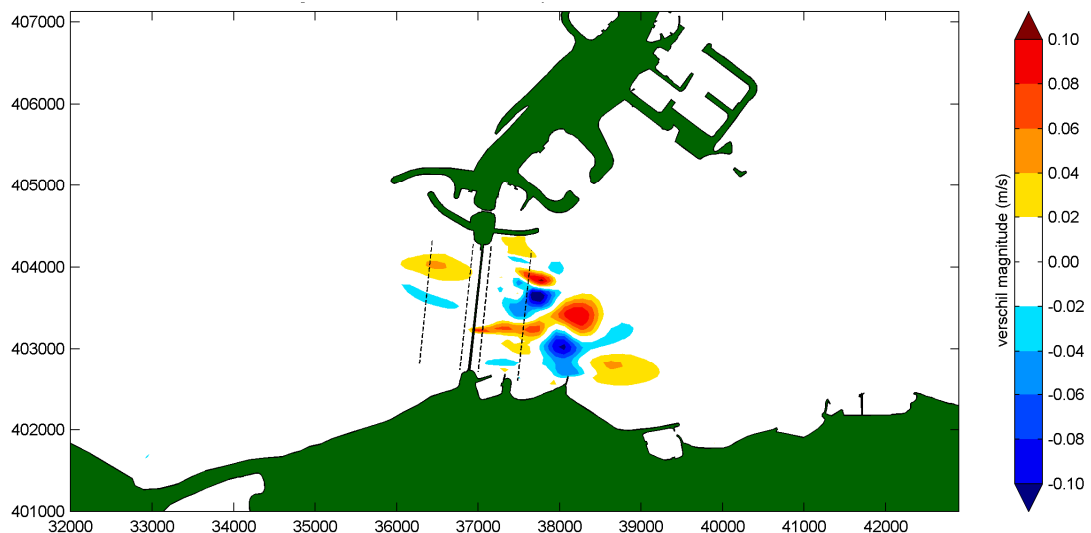


Figure 4.4 Difference in velocity magnitude between Case 3 (turbines in RP8 and RP10) and Case 1 (no turbines).
The dashed lines represent a distance of 100m from the barrier and the edge of the bed protection at 600m.

Additionally to the velocity magnitude, an assessment is made of the velocity direction. The deviation in velocity direction for the situation with turbines and without turbines is approximately 10° for both situations. This change in velocity direction occurs mainly at low head differences. During large head differences, no change in flow direction is observed for the situation with or without turbines. Figure 4.5 shows a time instant during low head of the difference in velocity angle for the situation with (blue arrows) and without turbines (red arrows).

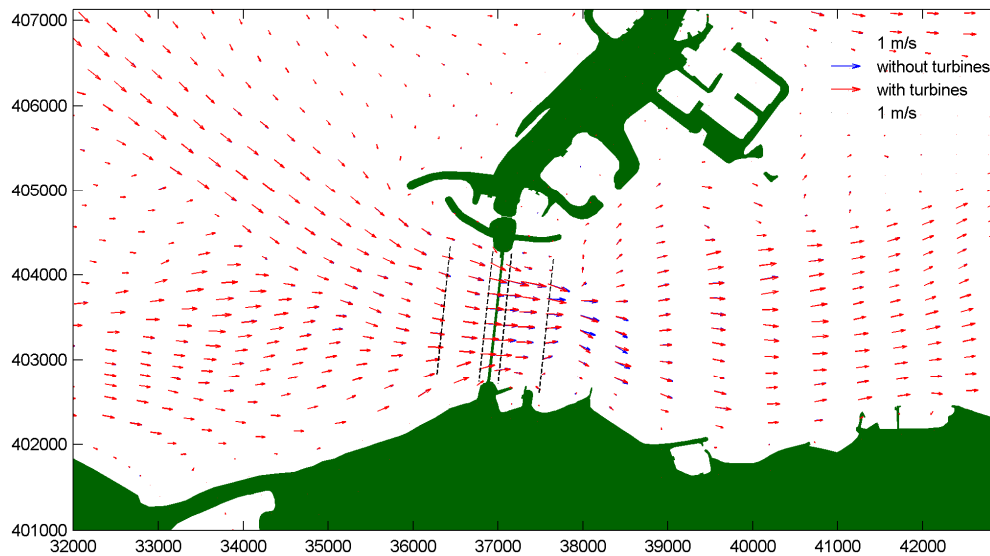


Figure 4.5 Velocity angle during flood for a small head difference over the barrier. The dashed lines represent a distance of 100m from the barrier and the edge of the bed protection at 600m.

4.3 Conclusion

From the large-scale modelling that has been performed, the impact of the tidal turbines on the flow patterns in the Roompot Channel has been investigated. In the simulations a conservative discharge coefficient has been used for the turbines in Roompot 10 (after [8]), as details of the design for the turbines in Roompot 10 are presently unknown.

From the modelling, it is concluded that the changes in velocity magnitude can reach up to 10cm/s when turbines are operating in Roompot 8 and Roompot 10 for a head difference of 90 cm over the barrier. For the turbines installed in Roompot 8 only, changes up to 3cm/s are observed. The flow direction remains unchanged at high head differences, while for small head differences changes up to 10° are seen for both cases.

5 Subject 4: Impact on bed protection

In this assessment, an investigation was carried out into the potential effect of the tidal turbines on the bed protection (see Figure 5.1). To assess the impact, the detailed flow fields near the bed simulated by the CFD model (see Section 3.2) for Gate Roompot 8 are used.

State-of-the-art bed protection formulas only use depth-averaged flow parameters to assess the stability of the bed protection. Due to the complex nature of the flow, a dedicated study was defined to develop a new stability formula to assess the impact near the bed based on flow information near the bed. The development of this new stability formula was carried out by Thieu Stevens in his M.Sc. Thesis for the TUDelft [4]. This Chapter describes briefly his research together with some additional modelling results, after which a conclusion is drawn on the impact of the tidal turbines on the (granular) bed protection.

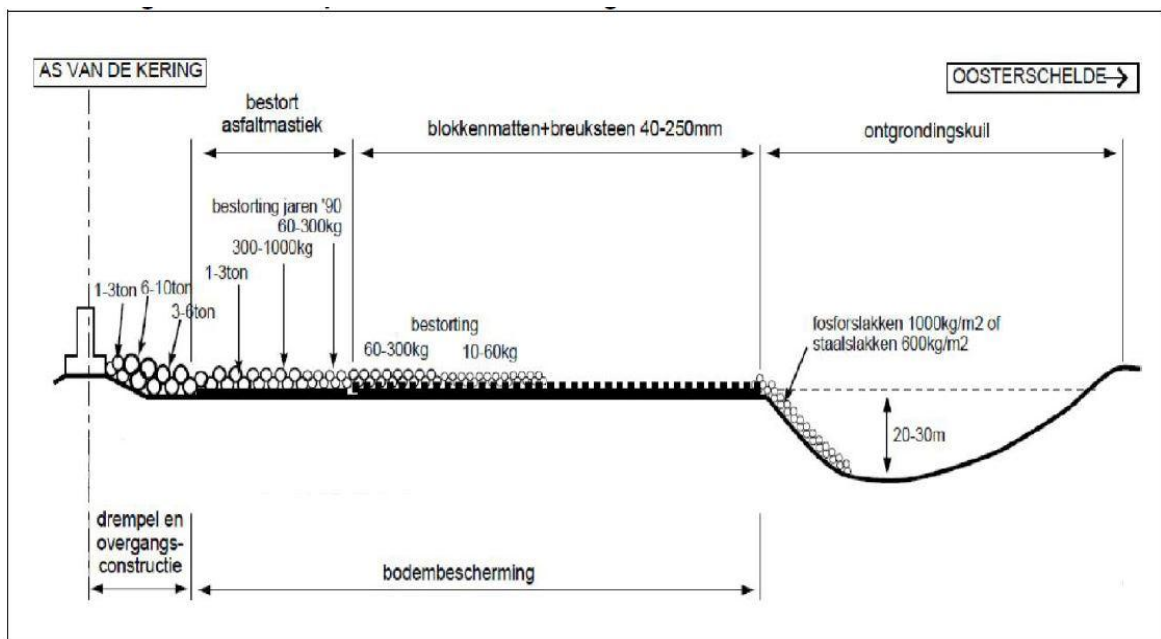


Figure 5.1 Sketch of the bed protection on the Eastern Scheldt side of the barrier (source: Rijkswaterstaat).

To develop the new stability formula based on the hydraulic parameters near the bed, a numerical model validation was performed. This validation was based on the tests of Jongeling et al., 2003 [10]. The results of this validation and the developed stability formula were used to assess the impact on the bed protection near the Eastern Scheldt Barrier.

5.1 Changes in flow patterns due to the turbines

The changes of the mean velocity and velocity fluctuations near the Eastern Scheldt barrier were investigated by means of the CFD model introduced in Section 3.2. The mean velocity for the situation without turbines and with turbines is shown in Figure 5.2. From this figure it becomes clear that the recirculation zone is different for the situation with turbines than for the situation without turbines, where a stronger return flow is present. Next to that, the energy extraction by the turbines is clearly visible from the velocity deficit in case of turbine operation.

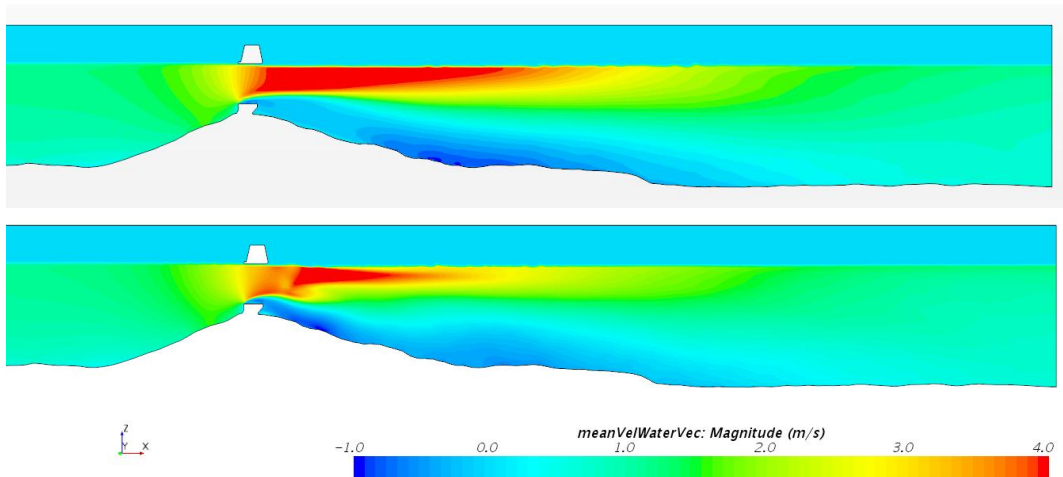


Figure 5.2 Mean velocity for a vertical cross section in between the turbines for Case 4 without turbines (top figure) and with turbines (lower figure).

In Figure 5.3, the mean kinetic turbulent energy is shown for the situation with turbines and for the situation without turbines. In these figures it is seen that the turbulent kinetic energy is generally lower for the case with turbines than for the case without turbines. When looking at Figure 5.2, a much stronger shear layer between the top and the bottom part of the water column is present for the cases without turbines than for the cases with turbines. Due to the detachment of the flow from the sill, this strong shear zone develops in the situation without turbines, while this shear zone is less strong when the turbines are present. This results in a lower turbulent kinetic energy for the cases with turbines than for the cases without turbines.

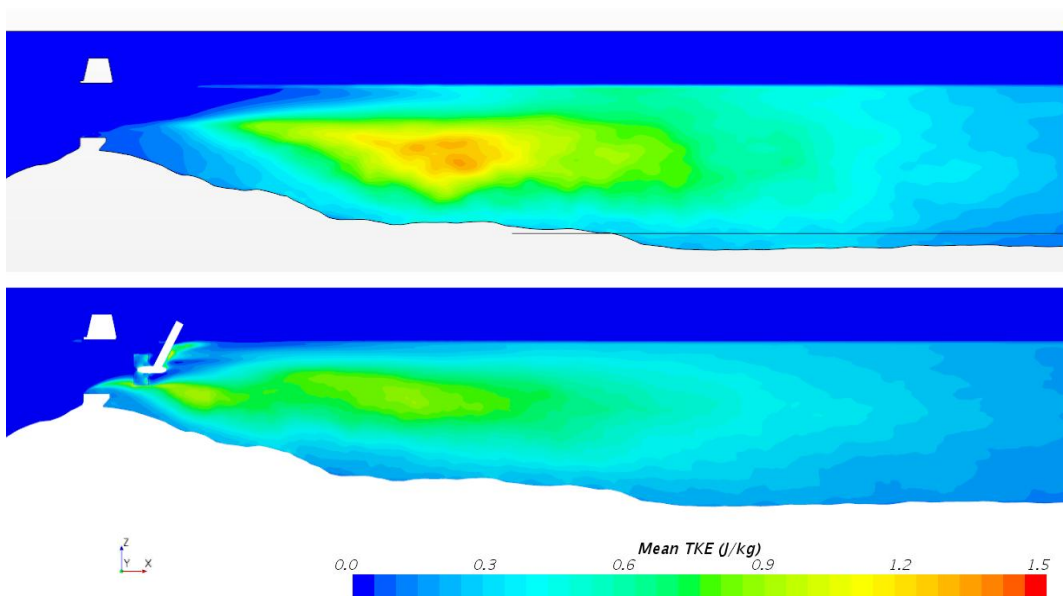


Figure 5.3 Mean turbulent kinetic energy for a vertical cross section through the turbines for Case 4 without turbines (top figure) and with turbines (lower figure).

A lower turbulent kinetic energy level results in a lower forcing on the bed protection. The adapted Shields formula as proposed by Jongeling [10], includes the turbulent kinetic energy:

$$\psi_{tot} = \frac{(u + 6\sqrt{k})^2}{\Delta g d}$$

From this formula follows that in case of a lower turbulent kinetic energy (k), the movability parameter (ψ_{tot}) also reduces.

Stevens [4] investigated the impact on the bed protection by using the hydraulic parameters of the flow near the bed. Based on his analysis, the mean velocity and the velocity fluctuations near the bed are assessed at a distance of 100m from the barrier. By using a generalized stability formula from Hofland [11], an assessment is made on the movability of the granular bed:

$$\psi_{tot} = \frac{(C_b(\bar{u} + \tilde{u}')^2 + (C_m(\bar{a} + \tilde{a}')d)_{max}}{\Delta g d}$$

In this formula it is observed that the mean velocity (\bar{u}), the velocity fluctuations (\tilde{u}'), the mean acceleration (\bar{a}) and the acceleration variation (\tilde{a}') determine the movability of the bed. Here, the fluctuation terms (\tilde{u}') and (\tilde{a}') are a measure for the turbulence.

5.2 Flow fields near the bed at 100m from the barrier

To be able to relate the velocity differences to the real velocities near the bed, the mean absolute velocity at 100m from the barrier is shown in Figure 5.4 for the Cases 2 and 4.

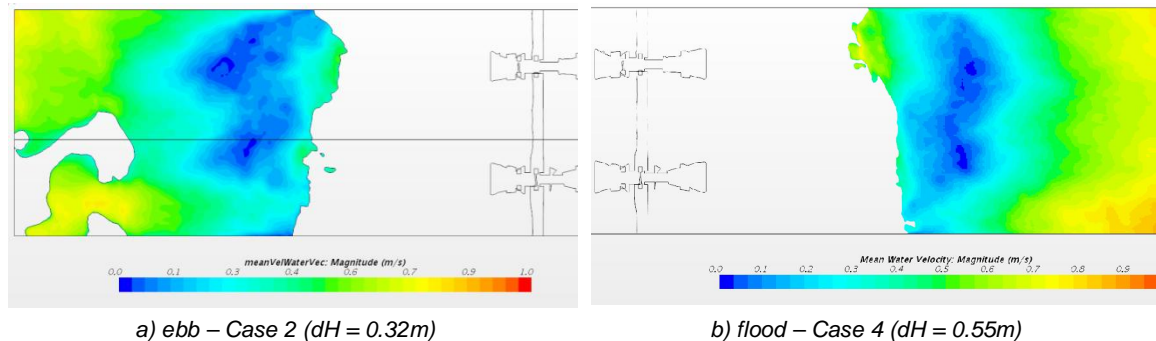


Figure 5.4 Mean absolute flow velocity downstream of the turbines at 100m from the barrier for the cases 2 and 4. Note that the model width is 90m.

Figure 5.5 shows the difference between the mean longitudinal velocity (U_x) for the situation with turbines and without turbines for a head difference of 32cm during ebb (Case 2) and 55cm during flood (Case 4). Near the turbines large differences are found. These differences reduce further away from the barrier. At a distance of 100m from the barrier and near the bed, where the granular bed protection begins, patches with higher and lower mean flow velocities are observed.

Figure 5.5 can also be used to address the concern of a downward facing jet induced by the turbines, which might have a negative impact the bed protection. This concern is based on the experience with partially closed gates. For Ebb, Case 2, the increase in flow velocity under the turbine in the first 100 m from the barrier is generally less than 0.5 m/s and located in a zone at mid depth. For Flood, Case 4, the increase in flow velocity is initially larger than 0.5 m/s and overall located in a zone lower in the water column. However, the velocity difference has decreased to well below 0.5 m/s when the zone reaches the bed at approximately 30 m from the barrier. These zones represent only a shift in the mean flow field. There is no indication of a downward facing jet due to the turbines.

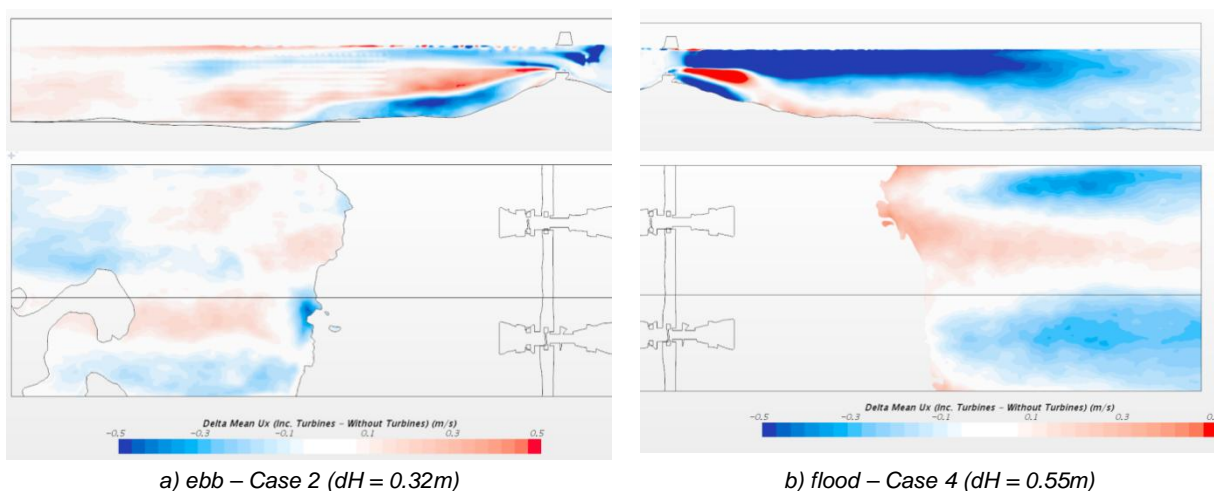


Figure 5.5 Difference in mean longitudinal velocity for a vertical cross section through turbine 2 (top) and a horizontal cross section near the bed (lower figure). The horizontal black lines represent the locations of the cross sections.

In Figure 5.6, the difference in velocity fluctuations are shown. From these figures it becomes clear that for the situation with turbines generally smaller velocity fluctuations are present than for the situation without turbines. This is in line with the lower turbulent kinetic energy for the situation with turbines that is seen in Figure 5.3.

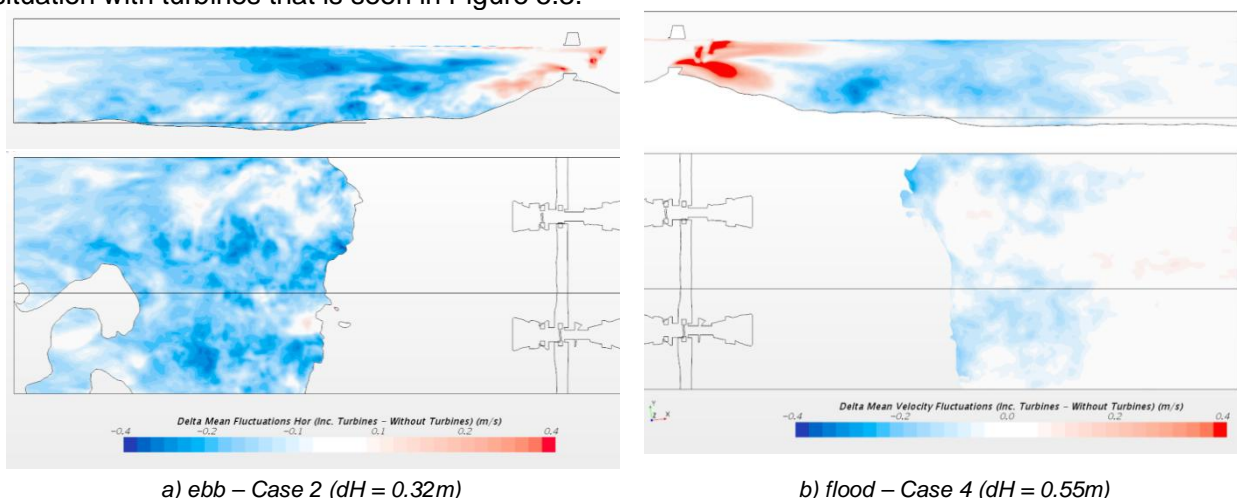


Figure 5.6 Difference in mean velocity fluctuations for a vertical cross section through turbine 2 (top) and a horizontal cross section near the bed (lower figure). The horizontal black lines represent the locations of the cross sections.

Table 5.1 shows the averaged differences for the situations with turbines and without turbines near the bed at 100m from the barrier. In this table, it is seen that the mean velocity and the velocity fluctuations drops slightly for almost all cases due to the turbines in Gate 8.

Table 5.1 Averaged differences in velocity and velocity fluctuations at 100m from the barrier near the bed.

	Case	Head [m]	Mean velocity [m/s]	With turbines – without turbines	
				Mean velocity [m/s]	Velocity fluctuations [m/s]
Ebb	1	-0.19	-0.26	-0.02	-0.11
	2	-0.32	-0.29	-0.03	-0.15
Flood	3	0.21	0.25	0.02	-0.04
	4	0.54	0.31	-0.08	-0.04

Based on the general stability formulas, lower flow velocities and velocity fluctuations lead to a lower forcing on the bed protection. It has to be noted that these results in Table 5.1 are averaged results. At some locations, the velocities and velocity fluctuations slightly increase. However, in general a decreasing trend is observed in mean velocity and velocity fluctuations near the bed.

5.3 Conclusions

The impact of the tidal turbines on the granular bed protection has been assessed by studying the changes in mean velocity and turbulence intensity for the situation with and without tidal turbines. In this assessment, it is seen that the hydraulic forcing on the bed protection changes in case tidal turbines are installed. The simulations have shown that for some locations, the turbulence intensity can be lower when tidal turbines are installed, as the turbines reduce the strength of the turbulent eddies coming from the sill. At other locations, the velocities and velocity fluctuations slightly increase.

It is important to state that for the simulated conditions no downward facing jet due to the turbines was observed, that might have a negative impact on the bed protection.

Although in general a decreasing trend was observed in mean velocity and velocity fluctuations near the bed, locally some increase is possible. Overall the impact on the bed protection is considered to be neutral.

6 Subject 5: Morphological effects in the Eastern Scheldt

In addition to the large-scale flow patterns discussed in Chapter 4, an assessment has been made of the potential morphological changes in the Eastern Scheldt due to the installation of the tidal turbines. In this assessment, Guijt [5] performed numerical modelling simulations using the Delft3D modelling suite to include sediment transport.

In this assessment, the sedimentation and erosion of the Roggeplaat, Neeltje Jans and the Galgenplaat has been assessed. This investigation is closely related to the further morphological modelling study performed by the TUDelft (Gatto). Here we focus on the results obtained by Guijt.

To study morphological effects a Delft3D flow model is used (see Figure 6.1) as a basis in this assessment. Unlike WAQUA (see Chapter 4) Delft3D had no options to include different discharge coefficients for ebb and flood. But similar to the WAQUA model, the Delft3D model has been calibrated on water level measurements from the standard monitoring stations in the Eastern Scheldt basin. The Delft3D model represents the tidal dynamics in the Eastern Scheldt well, with a maximum RMS error of 8 cm for the water level at Marollegat.

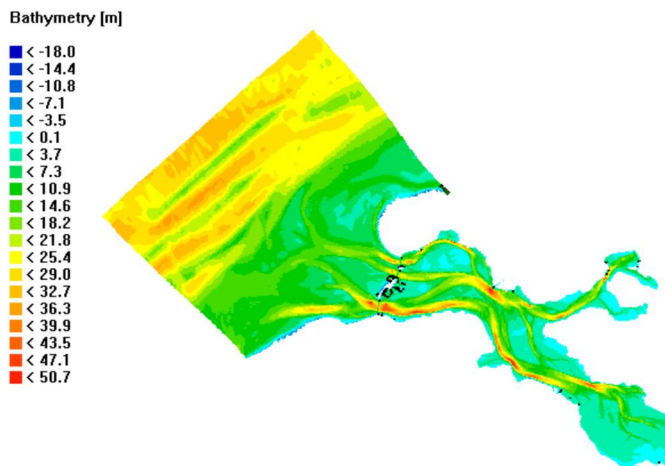


Figure 6.1 Bathymetry and outline of the Delft3D model that has been used for the morphological assessment.

6.1 Roll-out scenarios

To assess the impact, different scenarios for the installation of tidal turbines in the Eastern Scheldt barrier have been assessed. The selected cases were selected in consultation with Tocardo and are listed in Table 6.1:

Table 6.1 Assessed scenarios. The numbers indicate the number of openings including turbines.

	Roompot	Schaar	Hammen
Near future	2 (Gate 8+10)		
Maximum rollout	9	4	4
Partially roll-out Roompot	9		
Partially roll-out Schaar		4	
Partially roll-out Hammen			4

6.2 Relative effect with respect to Sea Level Rise

Due to the increased resistance of the barrier by the installation of tidal turbines, the tidal range in the basin decreases. This results in a rise of the level of mean low water (MLW). To assess the implication of this rise in MLW, the results are presented against sea level rise scenarios, which also cause an increase in MLW.

De Ronde et al. [12], defined 3 scenarios for mean sea level rise in the Eastern Scheldt based on KNMI climate change scenarios. Here, the middle scenario is selected for the analysis. In this scenario, the future sea level rises at 4.17mm per year between 1990 until 2050 (the present rate is 2 mm /yr). Table 6.2 shows the results of the installation of the tidal turbines in terms of years of sea level rise.

Table 6.2 Change in mean low water level due to the turbines for the near future and the max roll-out scenario.

	MLW rise	Sea level rise
	[cm]	[years]
Near future	0.5	1.1
Max roll-out	2.4	5.8

6.3 Morphological impact

Due to the construction of the Eastern Scheldt Barrier 'sand demand' exists in the Eastern Scheldt, see Section 1.1. By an increased resistance in the barrier due to the installation of tidal turbines, this process might accelerate. Guijt [5] assessed the degradation of the tidal flats for the different scenarios (see Table 6.3). From this, it followed that the additional flat degradation is about 0.1% when tidal turbines are installed in the Gates Roompot 8 and Roompot 10. This increases to 0.7% when turbines are installed in 17 gates.

Table 6.3 Tidal flat development for the near future and maximum roll-out scenario.

	MLW rise [cm]		Area loss [ha]		Area loss [%]	
	near future	max roll-out	near future	max roll-out	near future	max roll-out
Roggeplaat	0.3	1.6	1.0	5.2	0.1	0.4
Neeltje Jans	0.3	1.6	0.2	1.3	0.1	0.5
Galgenplaat	0.4	2.3	1.3	13.1	0.1	1.4
All			2.5	19.5	0.1	0.7

6.4 Conclusion

A large-scale assessment has been made of the effects of tidal turbines in the Eastern Scheldt on the hydrodynamic and morphological changes. In this assessment, various scenarios have been addressed. The effect of tidal turbines in Gates Roompot 8 and 10 on the increase of the mean low water level is equivalent to about 1.1 year of predicted future sea level rise, which equals an intertidal area loss of about 0.1%.

7 Discussion on maximum allowable head difference over the barrier

Tocado expressed the wish to increase the maximum head difference for the operation of the tidal power plant from 60 cm and 80 cm during respectively ebb and flood according to the permit (indicated by “-60/+80”) to 90 cm for both conditions (indicated by ‘-90/+90’), for the Roompot 08 (operational) and Roompot 10 (planned) tidal power plants. RWS is willing to address such a request by Tocardo, provided that it can be shown that such an increase will not provide extra risks for the barrier. In this respect RWS has expressed its concern on the increase of flow velocities and turbulence, in particular with respect to the following aspects:

- Possible increase of turbulence due to the turbines;
- ‘Downward facing jet’ induced by the turbines;
- The effect of the turbines on the bed protection at 100 m or more from the barrier;
- Possible flow asymmetry in the Roompot due to the tidal power plants;
- Possible change of the large-scale flow pattern in the Roompot channel due to tidal power plants in the Gates Roompot 8 and Roompot 10.

Below, these concerns are addressed, based on the results of the studies summarized in this report.

Possible increase of turbulence due to the turbines. This concern is based on the expectation that the rotor blades of turbines may lead to additional turbulence, around and downstream of the turbines. Chapter 5 showed the following:

- For Case 4 (Flood, head difference dH is +52 cm) the CFD model showed that the turbines significantly reduce the maximum turbulent kinetic energy in the far wake, while locally near (and under) the turbines the turbulent kinetic energy has somewhat increased (see Figure 5.3). For Case 2 (Ebb, dH is -32 cm) the difference in mean velocity fluctuations due to the presence of the turbines in Figure 5.6 shows similar but smaller effects (though for a lower head difference). These cases are indicated by -32/+55 cm.
- Based on the -32/+55 cm results, a similar development of the turbulence levels is expected for the -90/+90 cm case of Gate Roompot 08.
- For Gate Roompot 10 it is expected that with a similar type of turbine, similar results for turbulence development will be found as for Gate Roompot 8.

Downward facing jet induced by the turbines. The concern of RWS is based on laboratory experiments² combined with practical experience that a partially closed gate may produce a downward directed main flow instead of the normal main flow along the water surface. This aspect can be addressed on the basis of the CFD model results.

- The turbines in Gate Roompot 8 do not lead to a downward directed flow for the cases investigated (-32/+55 cm). For Flood (Case) 4, see Figure 5.2, the main flow remains attached to the water surface, albeit spread over a greater depth. The return flow near the bed even increased up to 30 m from the barrier, but further away it is somewhat reduced. For ebb Case 2 the mean longitudinal velocity difference (U_x) due to the presence of the

² See the design document of the Eastern Scheldt Barrier [13]: During ebb a notable change in flow pattern may occur when that gate is closed for more than 30%. In that case, the main flow along the water surface with a horizontal eddy near the bed changes to a main flow directed downward along the bed (‘duikende straal’). Due to this phenomenon the maximum allowed head differences during ebb had to be reduced.

turbines in Figure 5.5 shows that the effects during ebb are similar but smaller (though for a lower head difference).

- Based on the -32/+55 cm cases it is expected that the differences in the vertical distribution of the flow become stronger for larger head differences. Therefore, separate simulations for -90/+90 (ebb and flood), with and without turbines would be required (4 additional CFD model runs) to address the risk of a downward facing jet for that particular case.
- Provided that for the tidal power plant in gate Roompot 10 the type of turbines and their relative position with respect to the sill is the same as for Gate Roompot 8, a similar hydrodynamic behaviour is expected in Roompot 10. However, when the design of the power plant of Roompot 10 is changed during optimization, new simulations for this design would be required.

The effect of the turbines on the bed protection at 100 m or more from the barrier. These effects have been assessed in Chapter 5 on the basis of the CFD modelling for Gate 8 with head differences of -20/+20 and -32/+55 cm.

- Generally, the CFD simulations showed a decreasing trend in mean velocity near the bed (2 – 8 cm/s) and velocity fluctuations near the bed (4 – 15 cm/s) at 100 m from the barrier, for Gate Roompot 8 (see Table 5.1).
- The simulations showed that for some locations in the investigated area, the turbulent velocity fluctuations can be lower when tidal turbines are installed, as the turbines reduce the strength of the turbulent eddies coming from the sill. At other locations, the velocities and velocity fluctuations slightly increase.
- Although, locally some increase is possible. Overall the impact of the tidal turbines on the bed protection is considered to be neutral for the investigated cases in Roompot 8.
- The extrapolation of these results to -90/+90 cm is related to the first two aspects, the turbulence levels and the downward facing jet. This means that without further simulations for the -90/+90 cm cases no definitive answer can be given
- For gate Roompot 10 the conclusion depends on the design changes, as mentioned above.

Possible flow asymmetry in the Roompot due to the tidal power plants. With the term 'flow asymmetry' changes in distribution of the discharges over the gates of the Roompot section of the barrier is indicated. In Chapter 4 this is addressed on the basis of the WAQUA modelling.

- The turbines in Roompot 8 were implemented in the WAQUA model, based on the change in the ebb and flood discharge coefficient of Roompot 8 resulting from the CFD modelling for Cases 1 to 4. Thereby, it was assumed that these corrections apply for the entire range of head differences (no limitation to head difference in the model). In the results of the model simulations no appreciable increase in discharge in adjacent gates to Roompot 8 is observed for large head differences over the barrier due to the tidal turbines in Roompot 8, see Figure 4.2. Only at small head differences some effect may be visible, see Section 4.2.
- The same holds when a tidal power plants is added in Roompot 10, based on conservative estimates of the changes in ebb and flood discharge coefficients.
- Though this would agree with the observation that the upstream velocities do not change due to the turbines (Section 3.1.4), it remains to be seen if this is entirely correct. The flow bypassing will be addressed in more detail the New Delta project, mentioned in Section 1.4.3.

Possible change of the large-scale flow pattern in the Roompot channel due to tidal power plants in the Gates Roompot 8 and Roompot 10. From the investigation in Chapter 4, based on the WAQUA model, it is concluded that the change in depth-averaged flow is fairly small.

- In the Roompot channel a change in depth-averaged velocities of maximum 10 cm/s is visible for the situation with turbines in Roompot 8 and 10 for a head difference of 90 cm, compared to the reference situation without turbines, see Section 4.2.
- The flow direction remains unchanged at high head differences, while for small head differences changes up to 10° are found.

In summary, the tools developed and applied in the investigations reported in the previous chapters seem to be adequate to address the impact of tidal turbines on the various aspects of flow velocities and turbulence mentioned above. Even though the effects of the tidal power plant in Roompot 8 are fairly mild, the extrapolation of the CFD results of the investigated cases of -20/+20 cm and -32/+55 cm for Gate Roompot 8 to an increased head difference of -90/+90 cm is not feasible. For license purposes it is relevant to prove by additional simulations for -90/+90 cm (ebb and flood), with and without turbines that there is not the smallest risk at plunging jet flow patterns or danger for the bed protection. Furthermore, when the design of the tidal power plant in Gate Roompot 10 is changed such that the type of turbines and/or their position with reference to the sill is different when compared to Roompot 8, new simulations for this will be required as well.

8 Summary

This report comprises the results of 6 different assessments on the potential effects of the installation of tidal turbines in Gates Roompot 8 and Roompot 10 of the Eastern Scheldt Storm Surge Barrier. This Chapter summarizes the six assessments, and describes the general conclusions. More detailed information can also be found in the separate reports (see Chapter 9).

1 Impact on tidal ranges in the Eastern Scheldt of turbines in Gate Roompot 8

From the analysis of the water level measurements in the Eastern Scheldt, including one year of turbine operation in Gate Roompot 8, no clear effect of the tidal turbines on the tidal range in the Eastern Scheldt could be detected. To improve the analysis, longer series of water level measurements with turbine operation would be required. However, the effect of the tidal turbines in Gate 8 will be significantly lower than the natural variation of the water levels, due to for instance the 18.6 year tidal cycle (9-14 cm), storm surge frequency and barrier operation or long-term effects of the Eastern Scheldt Barrier construction and related morphological developments.

2 Influence on discharge capacity of the barrier

A. Derived from current measurements in Gate Roompot 8

Prior to the installation of the tidal turbines in Gate Roompot 8, current measurements were performed of the flow through the barrier. After deployment of the turbines a new set of current measurements was obtained. However, it turned out that these measurements could not be used to provide a sufficient reliable estimate of the impact of the tidal power plant on the discharge through Gate Roompot 8 of the Eastern Scheldt Barrier due to the lack of overlap in measurement cells and the large uncertainty in the measurements. Furthermore, during ebb, the Gate opening is in the wake of the tidal turbines, which increases the inaccuracy of the discharge estimate significantly.

Note that no change in the upstream flow was observed from a comparison of measurements when the turbine was operational and in stall mode, effectively a non-operational condition.

B. Derived from CFD computations for Gate Roompot 8

In an alternative approach detailed CFD models were used, which were validated against the available velocity measurements, and the power and the thrust measurements. Based on the validated CFD model more reliable estimates of the changes in discharge capacity due to the presence of the tidal turbines in Gate Roompot 8 were obtained. The discharge capacity of Gate Roompot 8 hardly changed during flood and decreases by about 5% during ebb. The main reason for this is the fact that the turbines are positioned upstream of the barrier sill during ebb and sufficiently far downstream of the barrier sill during flood. During ebb, the turbines are blocking the flow towards the barrier, while during flood the influence of the turbines on the flow becomes effective after the flow has passed the narrowest cross section of the gate (above the sill).

3 Impact on flow patterns in the Roompot (turbines in Gate Roompot 8 and 10)

From the large-scale modelling with the ScalOost WAQUA model, the impact of the tidal turbines on the flow patterns in the Roompot Channel has been investigated. In the simulations the discharge coefficients from the CFD analysis were used for Gate Roompot 8, while conservative discharge coefficients were used for the turbines in Roompot 10 because its design is not finished yet.

From the modelling results it is concluded that the changes in velocity magnitude can reach up to 10cm/s when turbines are operating in Roompot 8 and Roompot 10 for a head

difference of 90 cm over the barrier. For the turbines installed in Roompot 8 only, changes up to 3cm/s are observed. The flow direction remains unchanged at high head differences, while for small head differences changes up to 10° are seen for both cases.

4 Impact on bed protection

The impact of the tidal turbines on the granular bed protection has been assessed by studying the changes in mean velocity and turbulence intensity for the situation with and without tidal turbines. It was found that the hydraulic forcing on the bed protection changes when tidal turbines are installed. The simulations have shown that for some locations, the turbulent velocity fluctuations can be smaller when tidal turbines are installed, as the turbines reduce the strength of the turbulent eddies coming from the sill. At other locations, the velocities and velocity fluctuations slightly increase.

It is important to state that no downward facing jet due to the turbines was observed, that might have a negative impact on the bed protection.

Although in general a decreasing trend was observed in mean velocity and velocity fluctuations near the bed, locally some increase is possible. Overall the impact on the bed protection is considered to be neutral.

5 Morphological effects in the Eastern Scheldt (turbines in Gate Roompot 8 and 10)

A large-scale assessment has been made of different scenarios of tidal energy extraction in the Eastern Scheldt and the impact on the tidal flats. For the case of tidal turbines in Gates Roompot 8 and 10 the increase of the mean low water level is equivalent to about 1.1 year of future sea level rise, which equals an intertidal area loss of about 0.1%.

Based on the above information a discussion was held in Chapter 7 on the potential increase of the maximum allowable head difference over the barrier. The result of this discussion is summarized below.

6 Increase of operational head

The tools developed in the investigations reported seem to be adequate to address the impact of tidal turbines on the various aspects of flow velocities and turbulence for which RWS expressed its concern. The effects of the tidal power plant in Roompot 8 (operating under the -60/+80 cm condition) are fairly mild, and any environmental impact will be relatively small. It is expected that the impact for an increased operational head difference of -90/+90 cm will still be limited. However, for license purposes it is relevant to prove by additional simulations for -90/+90 cm (ebb and flood; with and without turbines) that there is not the smallest risk at plunging jet flow patterns or danger for the bed protection. Once the licence for the increased operational head difference is obtained, it is good practice to verify how accurate the simulation actually are. This can be carried out based on the standard monitoring practice. Furthermore, when the design of the tidal power plant in Gate Roompot 10 is changed when compared to Roompot 8, new simulations for this will be required as well.

9 References

9.1 Reports used for this summary report

- [1] Moerman, E; “*Eastern Scheldt Tidal Power – impact on tidal range due to tidal turbine installation*”, Deltares report ref: 11200444-000-HYE-0014, dated August 2018 (see Appendix A)
- [2] Verbruggen, W; “*Analysis ADCP data Eastern Scheldt Barrier with and without turbine deployment*”, Deltares report ref: 11200444-000-HYE-0008, dated August 2018. (see Appendix B)
- [3] O’Mahoney, T; “*CFD simulations of the Eastern Scheldt Barrier with and without tidal turbines – validation study and determination of discharge coefficients*”, Deltares report ref: 11200119-003-HYE-0004, dated August 2018. (see Appendix C)
- [4] Stevens, T; “*The prediction of stone stability by a three-dimensional eddy resolving simulation technique*”; M.Sc. Thesis TUDelft, dated July 2018. (see Appendix D)
- [5] Guijt, K; “*Impact of Tidal Energy Extraction in the Eastern Scheldt Storm Surge Barrier on Basin Hydrodynamics and Morphology*”, M.Sc. Thesis TUDelft, dated January 2018. (see Appendix E)

9.2 Additional references

- [6] Weisscher, V; Bijlsma, A.C.; “*Oosterschelde Tidal Powerplant Roompot 8 Meetprogramma*”, documentnummer: S.15002, rev. 1, dated 17 July 2015
- [7] Van der Kaaij, T; “*Oosterschelde WAQUA model 5e generatie – Modelopzet, kalibratie en validatie*”, Deltares report ref: 1220073-006-ZKS-0003, version 2, dated December 2015
- [8] De Kleermaeker, S.H.; Twigt, D.J.; “*Berekeningen getij-reductie in de Oosterschelde door getij-turbines in de Oosterscheldekering*”, Deltares report ref: 1202135-000-ZKS-0009, dated March 2010
- [9] Dillingh, D.; *Veranderingen in gemiddelde zeeniveaus in de Nederlandse kustwateren*. Deltares rapport 1206182-000-ZKS-0003, 2013. In opdracht van Rijkswaterstaat Waterdienst
- [10] Jongeling, T.H.G., Blom, A., Jagers, H.R.A., Stolker, C., and Verheij, H.J. (2003). Ontwerpmethodiek granulaire verdedigingen; rapport schaalmodelonderzoek, numerieke simulaties en bureaustudie. Report Q2933, Delft Hydraulics.
- [11] Hofland, B. (2005). Rock & Roll - Turbulence-induced damage to granular bed protections. PhD thesis, TUDelft.
- [12] De Ronde, J.G. , J.P.M.Mulder, L.A. Van Duren, and T.J.W. Ysebaert. Eindadvies ANT Oosterschelde. Deltares rapport 1207722-000-ZKS-0010, 2013.
- [13] Rijkswaterstaat (1989). Design document Storm Surge Barrier Eastern Scheldt. Book 2 Hydraulic engineering works (In Dutch: Ontwerpnota Stormvloedkering Oosterschelde; Boek 2, De waterbouwkundige werken)

